A STUDY INTO THE EFFECTS OF ELECTRIC FIELDS AND CURRENTS ON THE AGING AND QUENCH HARDENING OF STEELS

Final Report

Hans Conrad
January 15, 1993

U. S. Army Research Office

ARO Proposal Number 26825–MS
ARO Research Agreement Number DAAL03–89–K–0115

North Carolina State University
Raleigh, N. C. 27695

Approved for Public Release
Distribution Unlimited

MASTER COPY KEEP THIS COPY FOR REPRODUCTION PURPOSES

REPORT DOCUMENTATION PAGE

Form Approved
OMB No 0704-0188

1. AGENCY USE ONLY (Leave blank)	2. REPORT DATE	3. REPORT TYPE AND DATES COVERED
	January 15, 1993	

4. TITLE AND SUBTITLE A Study Into the Effects of Electric Fields and Currents on the Aging and Quench Hardening of Steels

5. FUNDING NUMBERS
DAAL03-89-K-0115

6. AUTHOR(S)
Hans Conrad

7. PERFORMING ORGANIZATION NAME(S) AND ADDRESS(ES)
N. C. State University
Raleigh, NC 27695

8. PERFORMING ORGANIZATION REPORT NUMBER

9. SPONSORING/MONITORING AGENCY NAME(S) AND ADDRESS(ES)
U. S. Army Research Office
P. O. Box 12211
Research Triangle Park, NC 27709-2211

10. SPONSORING/MONITORING AGENCY REPORT NUMBER
ARO 26825.21-MS

11. SUPPLEMENTARY NOTES
The view, opinions and/or findings contained in this report are those of the author(s) and should not be construed as an official Department of the Army position, policy, or decision, unless so designated by other documentation.

12a. DISTRIBUTION/AVAILABILITY STATEMENT
Approved for public release; distribution unlimited.

12b. DISTRIBUTION CODE

13. ABSTRACT *(Maximum 200 words)*

Studies were conducted on the effects of an internal electric current and an external electric field on the mechanical properties of metals and on solid state transformations therein, giving attention to the quench aging of a low-carbon steel and the hardenability of a tool steel. A continuous d.c. current of ~ 10^3 A/cm^2 increased the rate of quench aging at 80°C, whereas an a.c. current of the same magnitude and a frequency of 50–100 Hz dramatically suppressed the aging. An external electric field of ~ 14 kV/cm retarded the quench aging by altering the nature of the prcipitation process. Regarding hardenability, an external electric field of 1 kV/cm increased the hardenability of a tool steel by shifting the CT curve to longer times. It was further established during the present studies that high density d.c. pulses ($\geq 10^3$ A/cm^2 of ~ 100 μs duration) increased the plastic strain rate of metals by orders of magnitude, increased fatigue life and enhanced the rates of recovery and recrystallization but retarded grain growth. An external electric field of ~ 1 kV/cm reduced the flow stress during the superplastic

CONTINUED ON BACK

14. SUBJECT TERMS
Electric current, electric field, electric charge, quench aging, hardenability, plastic deformation, flow stress, dislocation
CONTINUED ON BACK

15. NUMBER OF PAGES
73

16. PRICE CODE

17. SECURITY CLASSIFICATION OF REPORT	18. SECURITY CLASSIFICATION OF THIS PAGE	19. SECURITY CLASSIFICATION OF ABSTRACT	20. LIMITATION OF ABSTRACT
UNCLASSIFIED	UNCLASSIFIED	UNCLASSIFIED	UL

13. Abstract (Continued)

deformation of 7475 Al, retarded grain growth and significantly reduced the cavitation. The effects of the electric current and external field on the various phenomena are explained in terms of their influence on the mobility of point (vacancies and solute atoms) and line (dislocation) crystal defects.

The present results demonstrate that electric currents and fields offer the possibility of either enhancing or retarding (and even suppressing completely) various phenomena, thereby providing potential for improving the efficiency of metal processing operations and/or the properties of the product.

14. Subject Terms (Continued)

mobility, recovery, recrystallization grain growth, fatigue, superplasticity, cavitation. Carbon diffusion, vacancy migration, cooling-transformation (CT) curve, Jominy end-quench, precipitate-free zone, dispersoid-free zone.

Final Report

ARO Proposal Number 26825–MS
Research Agreement Number DAAL03–89–K–0115

A STUDY INTO THE EFFECTS OF ELECTRIC FIELDS AND CURRENTS ON THE AGING AND QUENCH HARDENING OF STEELS

Hans Conrad
Materials Science & Engineering Department
North Carolina State University
Raleigh, N. C. 27695–7907

Contents

A STUDY INTO THE EFFECTS OF ELECTRIC FIELDS AND CURRENTS ON THE AGING AND QUENCH HARDENING OF STEELS

ABSTRACT

Studies were conducted on the effects of an internal electric current and an external electric field on the mechanical properties of metals and on solid state transformations therein, giving attention to the quench aging of a low-carbon steel and the hardenability of a tool steel. A continuous d.c. current of ~ 10^3 A/cm^2 increased the rate of quench aging at 80°C, whereas an a.c. current of the same magnitude and a frequency of 50–100 Hz dramatically suppressed the aging. An external electric field of ~ 14 kV/cm retarded the quench aging by altering the nature of the prcipitation process. Regarding hardenability, an external electric field of 1 kV/cm increased the hardenability of a tool steel by shifting the CT curve to longer times. It was further established during the present studies that high density d.c. pulses ($\geq 10^3$ A/cm^2 of ~ 100 μs duration) increased the plastic strain rate of metals by orders of magnitude, increased fatigue life and enhanced the rates of recovery and recrystallization but retarded grain growth. An external electric field of ~ 1 kV/cm reduced the flow stress during the superplastic deformation of 7475 Al, retarded grain growth and significantly reduced the cavitation. The effects of the electric current and external field on the various phenomena are explained in terms of their influence on the mobility of point (vacancies and solute atoms) and line (dislocation) crystal defects.

The present results demonstrate that electric currents and fields offer the possibility of either enhancing or retarding (and even suppressing completely) various phenomena, thereby providing potential for improving the efficiency of metal processing operations and/or the properties of the product.

Key Words

Electric current, electric field, electric charge, quench aging, hardenability, plastic deformation, flow stress, dislocation mobility, recovery, recrystallization grain growth, fatigue, superplasticity, cavitation. Carbon diffusion, vacancy migration, cooling-transformation (CT) curve, Jominy end-quench, precipitate-free zone, dispersoid-free zone.

Final Report

on

ARO Proposal No. 26825–MS: Research Agreement No. DAAL03–89–K–0115

A STUDY INTO THE EFFECTS OF ELECTRIC FIELDS AND CURRENTS ON THE AGING AND QUENCH HARDENING OF STEELS

INTRODUCTION

During the prior report period [1] it was established that internal electric currents and external electric fields can have significant effects on the mechanical properties of metals and alloys and on solid state transformations occurring therein. An electric current pulse of ~ 10^5 A/cm^2 for ~ 100 μs produced an increase in the plastic strain rate of the order of 10^5 with a resulting decrease in the flow stress of 5–40%. This direct effect of the drift electron flow was in addition to any produced by such side effects of the current as Joule heating or the pinch effect. Continued electric current pulses of similar magnitude and time period applied at a rate of 2 pulses per second increased the fatigue life of polycrystalline Cu by a factor of ~ 2 and enhanced the rates of recovery, recrystallization and retarded grain growth in a number of metals and alloys by factors of 20, 2 and 10 respectively. These effects of current pulsing are quite significant, considering that the current was "on" only 0.02% of the total time.

Regarding the application of an external electric field (where the specimen is one electrode of an electrostatic circuit), it was discovered that a field of ~ 1 kV/cm produced the following effects during the superplastic deformation of the 7475 Al alloy: (a) reduced the flow stress by 10–20%, (b) increased the strain rate hardening exponent slightly and (c) significantly reduced the cavitation throughout the thickness of the 1.6 – 1.8 mm thick sheet. It was also found for the

first time that an external electric field of 2–8 kV/cm retarded the recovery and recrystallization of metals and alloys and the quench aging of a low carbon steel and significantly increased the hardenability of steels.

The above results indicated that external electric fields and internal currents can provide electronic parameters or forces in addition to the external parameters of temperature and pressure (or stress) which are normally considered in materials behavior. The electric fields and currents may thus provide beneficial effects in the processing of metals and alloys. The objective of the present study was therefore to further investigate and evaluate the influence of electric fields and currents on the behavior of metals and alloys, giving attention to the quench aging and quench hardening of steels. This was deemed highly desirable, since only very limited work on this general subject was being conducted throughout the world. Some technological areas where the effects of electric fields and currents may be especially important are: (a) electromigration in microelectronic circuits, (b) power generating, transmission and switching systems, (c) high energy power sources including electromagnetic propulsion, (d) low and high temperature superconducting devices and (e) working and processing of metals, intermetallic compounds and ceramics.

ACCOMPLISHMENTS ON PRESENT GRANT

The work carried out on the present research grant (U. S. ARO DAALO3–89K–0015) for the period June 1, 1989 to October 31, 1992) is a continuation of that in [1]. Its objectives are to further investigate and evaluate the effects of internal electric currents and external electric fields on the behavior of metals, giving attention to the quench aging and quench hardenability of steels.

1. INFLUENCE OF ELECTRIC CURRENT

1.1 Continuous d.c. and a.c.

1.1.1 Quench Aging of a Low-Carbon Steel: That a continuous d.c. or a.c. current density of sufficient magnitude ($j > \sim 10^2$ A/cm^2) can influence the rate of precipitation in metal alloys has been reported by a number of investigators [2–8]. The results obtained are however somewhat contradictory. Erdmann-Jesnitzer et al [2,3] found that a d.c. current of $\sim 10^3$ A/cm^2 enhanced the rate of quench aging of Armco iron at 80°C, whereas a 50 Hz a.c. current of the same magnitude completely suppressed the aging. Somewhat similar behavior was observed by Koppenaal and Simcoe [4] for the aging of an Al–4 wt.% Cu alloy at 75°C in that a d.c. current enhanced the rate of precipitation, whereas a 25 Hz a.c. retarded it. No effect occurred for a 100 Hz a.c. current. In contrast, Shine and Herd [5] and Onodera et al [6] found that a d.c. current retarded the rate of precipitation in an Al–4 wt.% Cu alloy. Similar behavior was also noted for an Al–12 wt.% Zn alloy [7]. In the case of a.c. current, Onodera and Hirono [8] reported that it retarded the aging of the Al–12 wt.% Zn alloy at 30°C; the retarding effect decreased with increase in frequency in the range of 25 to 200 Hz. A slight increase in the rate of precipitation however occurred at 3000 Hz.

The retarding effect of the d.c. current was attributed by Onodera et al [6–8] to its enhancement of the migration of vacancies to grain boundaries, thereby reducing the number available for the diffusion of the solute atoms to form the precipitate. However, this model was unable to account for the frequency effect of the a.c. current.

Since an electric current can either enhance or retarding the aging process in alloys, this offers potential for exerting control of such phenomena during processing of an alloy. For example, an enhanced aging rate might be desired for

increasing the efficiency of the process, whereas a retardation or suppression would be desirable in the processing of non-equilibrium structures. It thus seemed highly desirable to investigate this phenomenon further, especially since to-date only limited work has been conducted on this subject and the results appear contradictory. This then provided the objective for the present investigation.

The quench aging of a low-carbon steel was chosen for study, because Erdmann-Jesnitzer and coworkers [2,3] had reported that at 80°C a d.c. current enhanced the rate of precipitation of carbon from solid solution and that an a.c. current of 50 Hz completely suppressed it as determined by resistivity measurements. Hardness measurements were however employed here to follow the aging process, in contrast to resistivity measurements which had been employed in all of the other studies on the effects of an electric current on aging [2–8]. For the quench aging of iron-carbon alloys, resistivity provides a measure of the amount of C remaining in solid solution (or in turn the amount that has precipitated) [9], whereas the hardness reflects the nature, size, shape and distribution of the precipitated particles [10,11]. The steel chosen for the present tests is similar in composition to that in [2,3]; therefore the two types of measurement should complement each other. Details regarding the present study are in process of being written for publication [12]; a summary of the more significant findings will be presented here.

The material employed in the present tests was a low-carbon steel sheet (50 μm thick) of the following composition in wt.%:

C	Si	Mn	P	S	Sol. Al	N
0.04	0.02	0.16	0.11	0.018	0.022	0.0024

Test specimens (2 mm wide x 40–50 mm long) were cut from the sheet in the

rolling direction, solutionized for 1 hr at 729°C, quenched in ice water and then aged for various times at 80°C with the following three conditions: (a) no current, (b) d.c. current of 10^3 A/cm^2 and (c) a.c. current of 10^3 A/cm^2 with frequency in the range of 25–1000 Hz. For the specimens aged with either the d.c. or a.c. current, the furnace temperature was adjusted to account for the Joule heating of 2–3°C.

Typical aging curves are shown in Fig. 1. The behavior without current exhibits two aging peaks similar to what was reported in [13]. The first peak is considered to reflect precipitation of $Fe_{16}C_2$ and the second precipitation of Fe_3C, based on the TEM observations of Leslie [10] and Keh and Leslie [11]. To be noted in Fig. 1 is that the d.c. current has four effects on the aging curve: (a) the general level of the hardness is lowered, (b) the time to reach the first peak is reduced, i.e. the aging rate is increased, (c) the first peak is considerably broadened and (d) the second peak is not distinct. The aging curve for the a.c. current of 100 Hz has a form similar to that for no current. However, for this frequency the overall level of the aging curve is significantly reduced. Moreover, the second peak appears to occur at a later time.

The form of the aging curves for the other a.c. frequencies was similar to that at 300 Hz; however, the general level of the curve depended on the frequency. This is illustrated in Fig. 2, which gives the maximum hardness (presumably representing the first peak) as a function of the frequency of the a.c. current. A sharp decrease in the maximum hardness occurs at a frequency in the range of 50–100 Hz, indicating a significant suppression of the aging process in this frequency range. A similar effect of frequency on hardness also occurred for the second aging peak. These effects of d.c. and a.c. current on the aging determined by hardness measurements are in qualitative accord with the resistivity measurements of Erdmann-Jesnitzer et al [2,3].

Of interest is the mechanism(s) by which the d.c. and a.c. currents affect the aging process. It is well established that resistivity measurements of the aging of a low carbon steel give directly the removal of C atoms from solid solution, whereas hardness measurements reflect the type, number, size, shape and distribution of the precipitate particles [9–11]. However, for the quench aging of a low-carbon steel, the time at which the maximum rate of decrease in resistivity occurs is the same as that at which the maximum rate of increase in hardness exists [9,11], thereby providing a means for comparing the results from the two types of tests. Considering the time at which the maximum rate of change in each measured property occurs, we find that the d.c. current reduced this time by a factor of ~ 2 in both the present hardness tests (Fig. 1) and in the resistivity measurements in [2,3].

One possibility for the increased rate of aging by the d.c. current is through an increase in the C-atom diffusion flux by electromigration. The total C-atom flux J_C is then given by

$$J_C = \frac{D_c c}{kT} \frac{\partial \mu_c}{\partial x} + \frac{D_c c}{kT} Z^* eE \qquad (1)$$

where $D_c = D_{o,c} \exp - \Delta H_c/kT$ is the C-atom diffusion coefficient, c the carbon concentration in solution (number per unit volume), $\partial \mu_c/\partial x$ the carbon chemical potential gradient, Z^*e the electronic charge on the C-atom in solution and $E = \rho j$ the electric field in the specimen with resistivity ρ and current density j. The first term on the right hand side of Eqn. 1 is the flux without current and the second that due to the current. If we assume that the rate of precipitation at a given time is proportional to the C-atom diffusion flux, we obtain by dividing Eqn. 1 by the first term

$$\frac{t_2}{t_1} = 1 + \frac{Z^* eE}{\partial \mu_c / \partial x} \qquad (2)$$

where t_2 is the time for the passage of a given number of C atoms without current and t_1 is that with the current. By taking $t_2/t_1 = 2$, $Z^* = 4$ [14], $\rho = 17$ $\mu\Omega$-cm (measured for the present low carbon steel) and $j = 10^3$ A/cm^2, we obtain for the chemical potential gradient $\partial\mu/\partial x = 6.8 \times 10^{-2}$ eV/cm. The spacing between the precipitates at maximum rate of hardness increase during the quench aging of rimmed steel at 60°C was ~ 500 Å [11]. Assuming a spacing of similar magnitude for aging at 80°C, Eqn. 2 gives $\Delta\mu \approx 3.5 \times 10^{-7}$ eV for the difference in chemical potential between the C in solution and the precipitate, which is here presumed to be $Fe_{16}C_2$. This value of $\Delta\mu$ indicates that the d.c. current has an influence on the precipitation of C during the quench aging considerably greater than expected from electromigration alone. This was also indicated in the results by Onodera and coworkers [6–8] for precipitation in Al alloys.

The decrease in the peak hardness which occurred with the d.c. current suggests that the current had an effect on the spacing of the precipitate particles, i.e. on the number of nucleation sites. Thus, although the current increased the growth rate of the particles, it also gave a decrease in the number of nuclei. One way the current might affect the number of nuclei is through an influence on vacancy migration, since the nucleation sites for C precipitation in α-iron are considered to be single or small clusters of vacancies [10,11].

Let us now consider the effect of a.c. frequency on the C precipitation process. Of immediate interest is a comparison of the mean jump frequency τ^{-1} of C atoms in α-iron at 80°C with the observed critical a.c. frequency ν_c at which the maximum suppression of aging occurs (50–100 Hz). The values of τ^{-1} derived from data taken from the literature (Table 1) for the diffusion of C atoms in α-iron

are given in Table 2. The listed values of τ^{-1} are of similar magnitude as ν_c, tending however to be somewhat larger. The difference however lies within the accuracy of the measurements of the diffusion coefficient. This then suggests that the effect of a.c. current on the aging process is through its effect on the diffusion of carbon. However, since the times for the first and second hardness peaks were not significantly influenced by the a.c. frequency in the range of 25 – 1000 Hz, it appears that the effect of the a.c. current was more on the nucleation or growth processes *per se* than on the diffusion of C in the α-iron. Hence, the suppression of the precipitation process could have resulted from either a difficulty in nucleation or a difficulty in growth of the precipitate particles.

Since the hardness decreased significantly at a critical a.c. frequency, the effect of the frequency of a.c. could be on the nucleation process, which is presumed to occur on single or small clusters of vacancies [10,11]. It is therefore also desirable to compare the jump frequency of vacancies in α-iron with the critical frequency for maximum suppression of the aging process, as well as the jump frequency of C atoms. However, only limited data are available for the migration of vacancies in α-iron (see Table 1) making the comparison difficult. By taking $D_0^v = 1\ cm^2\ s^{-1}$ and assuming that the jump frequency is equal to the critical a.c. frequency for maximum suppression of the aging process (~ 100 Hz), one obtains for the activation energy for vacancy migration in α-iron $\Delta H_m^v = 23.5$ kcal/mole, which is in reasonable accord with the values given in the literature (15.7–28.6 kcal/mole [15,16]), Table 2. Thus, the suppression of the aging process by the a.c. current could be due to its influence on the migration of vacancies (as related to their acting as nucleation sites), rather than to its influence on the diffusion of C in the α-iron matrix. The reason an optimum effect would occur

when the frequency of the a.c. current just matches the jump frequency of the vacancies is however not clear.

There also remains the question regarding the delay in the time for the second hardness peak (which is presumed to be due to the precipitation of Fe_3C [10,11]) at all frequencies of the a.c. current. Since the growth of the Fe_3C particles occurs at the expense of the previously precipitated $Fe_{16}C_2$ particles [10,11], it could be that the longer time for the second hardness peak results from an increased diffusion distance between the growing Fe_3C particles and the shrinking $Fe_{16}C_2$ particles. An increased distance would occur if a smaller number of $Fe_{16}C_2$ nucleation sites resulted from an influence of the a.c. current on nucleation.

It is evident from the above that the effect of an electric current on the quench aging of metals is not straightforward and that more work is needed to arrive at a better understanding of the mechanisms that are involved.

1.2 Effects of High-Density Electric Current Pulses

1.2.1 Plastic Deformation: Dislocation Mobility: The influence of a single electric current pulse of 10^3–10^6 A/cm^2 and ~ 100 μm duration on the flow stress of several FCC metals (Al, Cu, Ag) with differing stacking fault energy and a BCC transition metal (Nb) was investigated at 78–373K to determine the mechanism by which an electric current increases the plastic deformation rate at low homologous temperatures [17–20]. Since the strain rates produced by the current pulse were $\leq 10\ s^{-1}$, the results were analyzed employing the thermally activated dislocation motion concept, whereby the drift electrons assist the applied stress and thermal fluctuations for dislocation to overcome the obstacles to their motion; see Fig. 3. This gives for the ratio of the shear strain rate with the current $\dot{\gamma}_j$ to

that without current $\dot{\gamma}$ [20]:

$$\ln\left(\frac{\dot{\gamma}_j}{\dot{\gamma}}\right) \approx \ln\left(\frac{\dot{\gamma}_{oj}}{\dot{\gamma}_o}\right) - \left(\frac{\Delta U_j^* - \Delta U^*}{kT}\right) + \left(\frac{A_j^* - A^*}{kT}\right) b\,\tau^* + \ln\left[2\cosh\left(\frac{A_j^*.F_{ew}}{kT}\right)\right] \qquad (3)$$

where $\dot{\gamma}_o = N_{D,m} b\,\bar{s}\,\nu^* \exp(\Delta S^*/k)$ is the pre-exponential factor, $N_{D,m}$ the mobile dislocation density, b the Burgers vector, $\bar{s}$ the average distance the dislocation segment (l^*) moves per successful thermal fluctuation, ν^* the dislocation vibration frequency, ΔS^* the activation entropy, ΔU^* the energy to overcome the obstacle, A^* the activation area, τ^* ($= \tau - \tau_\mu$) the effective stress, F_{ew} the electron wind force and kT has its usual meaning. For polycrystals, $\dot{\gamma} = \bar{M}\,\dot{\varepsilon}$ and $\tau^* = \sigma^*/\bar{M}$ where $\bar{M}$ (~ 3) is the Taylor orientation factor and $\dot{\gamma}$ and σ are the true uniaxial strain rate and stress, respectively. The effects of the drift electrons on $\dot{\gamma}_o$, ΔU^*, A^*, ΔH^* and F_{ew} were determined by constant strain rate tensile tests in which current pulses of increasing magnitude were applied at different strain rates and temperatures; see for example [18]. The procedures and care which must be employed to eliminate the side effects of the current and to obtain the desired information are discussed in [17].

The effects of the drift electrons on the various parameters in Eqn. 3 are presented in Table 3 and illustrated in Fig. 4 for Cu and Nb. For FCC metals the largest contribution of the current is through the pre-exponential factor $\dot{\gamma}_o$, the effects on the other parameters being much less. Thus, we need to consider the influence of the current pulse on the components of $\dot{\gamma}_o$. Since $N_{D,m}$ is generally of the order of one-tenth of the total dislocation density, it is expected that the increase in $N_{D,m}$ is at most of the order of 10. This then leaves the influence of the current on the three remaining components $\bar{s}$, ν^* and ΔS^*. Additional work is needed to determine the effect of the current on these parameters. Worthy of note

is that ΔS^* enters into an exponential and therefore small changes in this parameter will produce large effects on $\dot{\gamma}_0$.

In the case of **BCC niobium**, the current pulse has a significant effect on the strain rate through both $\dot{\gamma}_0$ and ΔU^* (for BCC metals $\Delta U^* = 2\ H_K$, where H_K is the kink energy). However, the expected large increase in strain rate from the current pulse due to a decrease in H_K is countered by a significant decrease in the activation area A^*, so that the total contribution to the strain rate given by the change in ΔH^* ($= \Delta U^* - A^* b \tau^* - F_{ew} A^*$) is smaller than the increase in $\dot{\gamma}_0$.

Quantum mechanics or kinetic considerations [21–23] give for the electron wind force per unit dislocation length

$$F_{ew} = \alpha\, b\, p_F\, (j/e - n_e v_D) \qquad (4)$$

Alternately, one obtains from considerations of the specific dislocation resistivity [24–27]

$$F_{ew} = \rho_D\, e\, n_e\, j/N_D \qquad (5)$$

where α is a constant ranging between 0.1 and 1.0, b the Burgers vector, p_F the Fermi momentum, j the current density, e the electron charge, n_e the electron density, v_D the dislocation velocity, ρ_D the dislocation specific resistivity, N_D the total dislocation density. The experimentally-derived values for F_{ew} can then be compared with theoretical predictions through an electron wind push coefficient

$$B_{ew} = F_{ew}/v_e \qquad (6)$$

where $v_e = j/e\, n_e$. In turn, one can compare B_{ew} with the dislocation-electron drag coefficient B_e, which for Cu and Al has values of the order of 10^{-5} dyn-s/cm^2. Eqn. 4 yields $B_{ew} \approx 5 \times 10^{-5}$ dyn-s/cm^2 for the FCC metals Cu, Ag and Au by taking $\alpha = 0.25$, a common value; Eqn. 5 yields $B_{ew} \approx 10^{-4}$ dyn-s/cm^2 for metals in general.

The values of B_{ew} determined experimentally for the FCC metals Al, Ag and Cu and BCC Nb are presented in Fig. 5 as a function of temperature. For the FCC metals, the experimental values decrease with increase in stacking fault energy and are in reasonable accord with theoretical predictions. However, the indicated decrease in B_{ew} for Cu and Ag with temperature is not expected from the theory. In the case of the BCC transition metal Nb, the experimental B_{ew} is about an order of magnitude larger than predicted. One reason may lie in the accuracy of the experimental electronic parameters employed to calculate F_{ew} from Eqns. 4 and 5.

1.2.2 Fatigue: The effects of continued, high current density pulsing on the low cycle fatigue of polycrystalline Cu, [28,29] and α-Ti [30] were investigated. In the case of Cu, the current pulsing produced the following effects: (a) increased fatigue life by a factor of 2–3, (b) reduced intergranular cracking and (c) increased the homogenization of slip; see Fig. 6. The former two effects were attributed to the increase in slip homogenization. A model was developed to explain the effect of slip homogenization on fatigue life [29]. This gave for the fatigue crack growth rate

$$\frac{da}{dN} = C\left(\frac{\gamma_p}{A_A^{PSB} N^{PSB}}\right)^2 \qquad (7)$$

where C is a constant, γ_p the plastic strain range, A_A^{PSB} the area fraction of the surface containing persistent slip bands and N^{PSB} the linear slip band density. The increase in A_A^{PSB} and N^{PSB} by electropulsing was attributed mainly to a reduction in the stress required to activate dislocation sources at or near the surface.

In the case of α-Ti, the electropulsing reduced only slightly the initial rate of cyclic softening, but eliminated the secondary cyclic hardening which occurred in unpulsed specimens; see Fig. 7. This influence of the electropulsing was attributed to an enhancement of the dislocation velocity, which leads to a reduction in the effective stress σ^*. This in turn facilitates the occurrence of a low energy dislocation patch structure compared to a structure containing a large number of screw dislocations.

1.2.3 Recovery, Recrystallization and Grain Growth: Prior work [1] showed that electropulsing enhanced the rates of recovery and recrystallization of cold worked polycrystalline Cu. During the present period it was established that similar behavior occurred for polycrystalline Al and Ni_3Al and moreover that the electropulsing effect was relatively independent of purity for the Al and Cu [31]; see Fig. 8. Studies were also conducted on the effect of electropulsing on grain growth in Cu, focusing on the temperature regime where recrystallization was just complete [31,32]. Fig. 9 shows that in this regime electropulsing decreased the rate of grain growth in contrast to its enhancement of the rates of recovery and recrystallization. The retardation of grain growth in the electropulsed specimens was concluded to result from a reduction in the residual dislocation density in the freshly recrystallized grains, compared to the density in specimens annealed without current.

The influence of electropulsing on the rate of grain growth was analyzed in terms of the equation proposed by Li [33] for the case where the driving force decreases with time t due to the annihilation of dislocations

$$(dD/dt)^{-1} = 1/(k_G \Delta F_o) + (k_R / k_G)\, t \qquad (8)$$

where D is the grain size, k_G the grain boundary mobility constant, k_R a second-

order kinetics dislocation annihilation constant and ΔF_0 the driving force at zero time. Fig. 10 shows that the grain growth of Cu of two purity levels is in accord with Eqn. 8, the slope (= k_R/k_G) being larger for the electropulsed specimens and for a higher impurity content. The intercept (= $1/k_G\Delta F_0$) does not appear to be significantly influenced by either the electropulsing or the purity level. These results suggest that electropulsing mainly increases the dislocation annihilation rate constant k_R, which is in accord with the observed effect of electric current pulses on dislocation mobility discussed above. The effect of purity level is considered to result mainly from a decrease in the grain boundary mobility constant k_G, in keeping with the well known fact that impurities significantly reduce grain boundary mobility in metals [34].

In a study on the effect of electric current pulse duration (50–200 μs) and frequency of application (0.07 – 7 pulses per s) on grain growth in Cu [32] it was found that the ratio k_R/k_G was not significantly influenced by the pulse duration or frequency in the ranges considered. This suggests that either both k_R and k_G are equally affected by these current parameters or that the effect of the electric current already occurs in 50 μs and is governed more by a specific number of drift electrons rather than the total number.

2. INFLUENCE OF AN EXTERNAL ELECTRIC FIELD

During the prior report period [1] it was found that the application of an external electric field whereby the specimen is one electrode of an electrostatic circuit can affect solid state transformations and mechanical properties of metals and alloys. The objective of the present studies was to further characterize the effect and to evaluate the mechanism(s) involved.

2.1 Solid State Transformations

2.1.1 Quench Aging of a Low-Carbon Steel: It was found [35,36] that an

external electric field E of ~ 14 kV/cm (~ 7 kV across 0.5 cm) had the following effects on the quench aging curves of the same low-carbon steel sheet (0.04 C–0.16 Mn) employed in the studies discussed above for the effects of an electric current: (a) it reduced the hardness of the first aging peak more than the second so that only a single broad peak resulted (Fig. 11) and (b) it increased the activation energy derived for the time to reach maximum hardness from 0.68 eV to 0.85 eV (Fig. 12), the latter value being that for the diffusion of C in α-iron (see Table 1). The effect of the field became negligible when the grain size was increased from 13 to 56 μm.

TEM observations (Fig. 13) revealed that the major effect of the field on the microstructure was to increase the width of the relatively precipitate-free zone (PFZ) adjacent to the grain boundaries from < 0.1 μm at zero field to as much as 2 μm at E = 14 kV/cm. Moreover, with the field the precipitates in this zone mainly nucleated on dislocations (compared to homogeneously within the matrix in the grain interior) and their area density was considerably less and their size considerably greater (10 to 100 times) than in the grain interior, where their number and size was similar to that for aging without a field.

The reduction in hardness which resulted for aging with the field could be explained in terms of the increased width of the depleted zone adjacent to the grain boundaries, which is softer than the grain interior. It was proposed that the effect of the electric field on the aging process resulted from the charge at the specimen surface, which influences the vacancy concentration there in such a manner as to provide a driving force for their migration from the grain interior to the nearest grain boundary and thence along the boundaries to the surface; see Fig. 14. The role of the vacancies in the aging process is to provide nucleation

sites for the precipitation of carbon [10,11] and perhaps also be involved in the diffusion of carbon as a C-vacancy complex; see Table 1.

2.1.2 Hardenability of Steel: An exploratory study [37] established that the application of an external electric field of the order of ~ 1 kV/cm in the manner of Fig. 15 during the heat treatment of a tool steel increased its hardenability; see Fig. 16. The curves shown here are similar to Jominy end-quench curves, since the stainless rod to which the specimen was attached during the quench provided a slower cooling rate at that end compared to the rate at the tip of the specimen farthest from the attachment. Evident from Fig. 16 is that the effect of the field on the hardness is much greater during the quench than during austenitization.

The effect of cooling rate produced by various quench media on the response of the tool steel to the electric field is presented in Fig. 17, which gives a plot of the hardness taken within 1 mm of the specimen tip vs the measured average cooling rate between 800° and 500°C. The effect of the field was greatest at a cooling rate of ~ 20°C/s.

Also evident from Fig. 17 is that the response to the electric field depends on the composition of the steel, the effect being much greater for the 02 tool steel compared to the 4340 steel, the latter having the higher hardenability without an electric field. A chemical analysis of the two steels gave the following composition in wt.%:

Steel	C	Si	Mn	Cr	Mo	Ni	W	V	S	P	Cu
02	1.03	0.18	0.47	0.24	<0.05	0.036	<0.10	<0.10	0.030	0.035	0.14
4340	0.39	0.26	0.75	0.80	0.25	1.69	—	—	0.014	0.009	0.14

Optical microscopy and TEM revealed that the higher hardness produced by the

electric field was associated with an increased amount of martensite or bainite compared to pearlite.

The results of a subsequent, more definitive study [38] are presented in Fig. 18. In these tests the condition of a Jominy end-quench was more closely simulated in that during the quench only approximately 2.5 mm of the tip of the specimen was immersed in the quench medium. Also, the electric field was only applied during the quench, the quench medium being silicone oil at 25°C. The composition of the W1 steel used for these tests was determined to be in wt.%:

Steel	C	Si	Mn	Cr	Mo	Ni	W	V	S	P	Cu
W1	1.00	0.34	0.39	0.22	<0.05	0.11	<0.05	<0.01	0.018	0.012	0.19

Except for a slightly higher Si content, this steel has essentially the same composition as that of the 02 steel used in the earlier study [37].

The results in Fig. 18 confirm that the application of an external electric field during the quenching of a tool steel can increase its hardenability. The curves presented here are the average of two groups of specimens (30 mm long x 1.6 mm dia.) cut from different rods of the same lot of steel and heat treated at different times separated by about a month. The first group consisted of 7 separate specimens, the second of 13. Following quenching the specimens were sectioned lengthwise at the center and Vickers microhardness (200 g load) measurements taken every 1 mm along the length of the specimen starting from the quenched end. Typical scatter in the measurements is indicated by the error bars. Optical microscopy studies revealed the following structures along the specimen length:

E(kV/cm)	Distance from Quenched End				
	3 mm	4 mm	5	6	7
0	90%M–10% P	20%M–80%P	100%P	100%P	100%P
1	100%M	90%M–10%P	70%M–30%P	20%M–80%P	100%P

where M designates martensite and P pearlite. These structures are consistent with the hardness measurements.

To determine the effect of the electric field on the cooling-transformation (CT) behavior during the quench, 0.25 mm dia. chromel-alumel thermocouples were spot-welded at predetermined locations along the length of test specimens. The thermocouples were positioned at each mm along the length of the specimens, starting at 3–4 mm from their quenched tip and ending at 15–16 mm from the tip, giving a total of 8 positions. A duplicate set of specimens was employed for each thermocouple position, one for quenching with the electric field, the other without. Moreover, duplicate runs were conducted with and without the field for the first five positions from the tip. Cooling curves at each location were recorded by connecting the thermocouple to an X-Y recorder with a response time setting of 0.5 cm/s.

Examples of the cooling curves obtained with and without an electric field are given in Fig. 19 for three locations along the specimen length. The thermal arrests reflect the transformation of the austenite to pearlite. Evident is a delay in the transformation for the electric field. However, no effect of the field on the cooling curves occurred prior to the transformation, indicating that the influence of the field on the transformation was not an indirect effect through its influence on the cooling rate produced by the quench medium.

Fig. 20 presents the cooling-transformation (C-T) diagram constructed from the times for the beginning and end of the thermal arrests in cooling curves such as those of Fig. 19. Evident is that the electric field shifts the C-T diagram to longer times. The maximum shift for this alloy occurs at ~ 500°C, and amounts to ~ 36%. The CT diagram of Fig. 20 is in accord with the published isothermal transformation diagram for WI steel [39].

Of interest is the mechanism by which the electric field retards the eutectoid transformation. It is generally assumed that at low transformation temperatures the kinetics of pearlite formation is independent of the nucleation rate $\dot{N}$ [40] and that the time for a given fraction transformed is given by [41]

$$t = \frac{0.5\, d}{\dot{G}} \tag{9}$$

where d is the grain size and G the average growth rate. $\dot{G}$ is given by

$$\dot{G} = \frac{K\gamma D_{gb}}{(C_\gamma - C_\alpha)}\, S_{op}^3 \tag{10}$$

where K is a constant, γ is the austenite-pearlite interface energy, D_{gb} is the grian boundary diffusion coefficient, C_γ the carbon concentration in the γ phase, C_α the carbon concentration in the α phase and S_{op} is the pearlite spacing which maximizes the growth rate. S_{op} is given by

$$S_{op} = \frac{4\gamma}{\Delta S_f \Delta T_E} \tag{11}$$

where ΔS_f is the entropy change and ΔT_E the supercooling below the eutectoid temperature.

It is expected that the influence of the electric field on the CT curve, and in turn on hardenability, will be through its effect on one or more of the parameters in Eqns 10 and 11. One possible effect is on the migration of the quenched-in vacancies from the grain interior to the grain boundary and thence to the surface, similar to the situation discussed above for the quench aging of steel. A reduction in the concentration of vacancies at the grain boundaries resulting from their migration to the surface might retard the diffusion of carbon along the grain boundary needed to form the pearlite. A retardation would especially result if the

diffusion of the carbon occurred by means of a carbon-vacancy complex. The shift of 36% in the time for the beginning of the transformation at 500°C could thus result from either an increase of this magnitude in the pre-exponential D_0 of the diffusion coefficient or from an increase of 300–500 cal/mole in the activation energy for diffusion. Another possible effect of the field might be on the austenite-pearlite interface energy γ. Based on Eqns. 10 and 11, the observed shift in the C-T diagram could result from a 17% increase in the surface energy. Additional work is needed to determine whether the field affects either of these parameters and the degree. Furthermore, the studies to-date have been on relatively small diameter (1.6 – 3.0 mm) rods, where the effect of the field extended to the center of the specimen. Needed are tests on larger diameter specimens to determine the influence of the field on the depth to which the increase in hardenability occurs.

2.1.3 Annealing of Ni_3Al: An electric field of 1.9 kV/cm enhanced the rates of recovery and recrystallization of cold rolled (25%) Ni_3Al; see Fig. 21. This effect of an electric field is in contrast to that for Al and Cu, where a field retarded recovery and recrystallization [42]. This suggests that studies of the behavior of intermetallic compounds under an electric field may offer a means for arriving at a better understanding of the mechanisms involved. Also, electric fields offer the possibility of improving the efficiency of processing intermetallic compounds.

2.2 Superplastic Deformation

An exploratory study during the previous report period [1] revealed that an external electric field of the order of 1 kV/cm during the superplastic deformation of the 7475 Al alloy in uniaxial tension produced the following effects: (a) reduced the flow stress, (b) reduced strain hardening through an increase in the recovery rate, (c) increased slightly the strain rate hardening exponent and (d) significantly reduced the amount of cavitation. The present studies were

undertaken to define the behavior more thoroughly and to develop an understanding of the mechanism(s) involved. The results of these studies are presented in [43–46].

The present studies confirmed in more detail the results obtained in the earlier exploratory investigation. Moreover, they established the following additional features regarding the influence of an external electric field on the superplastic deformation of 7475 Al alloy:

(a) The maximum flow stress and the amount of cavitation depend on the polarity and magnitude of the electric field; see Figs. 22 and 23. It is here seen that a greater effect on both the reduction in flow stress and on cavitation occurs when the specimen is connected to the positive terminal of the power supply. In the case of the flow stress, reversing the polarity from specimen positive to specimen negative increased slightly the flow stress over that without an electric field. However, reversing the polarity in this manner did not increase the amount of cavitation over that for no field, but merely reduced its amount compared to when the specimen was connected to the positive terminal.

(b) Changes in microstructure in addition to reduction in cavitation which resulted from the application of an electric field of 2 kV/cm during the superplastic deformation of 7475 Al included the following:

  (1) A retardation of strain-induced grain growth, including that associated with dynamic recrystallization towards the end of the test, Fig. 24.

  (2) A slight increase in the width of the dispersoid-free zones (DFZ), Fig. 25. The DFZ occurred mainly at grain boundaries perpendicular to the tensile axis.

  (3) An increase in the Zn/Cu atom ratio in the DFZ.

(4) An increase in the size of the dispersoids at the sides of the DFZ's bounded by the grain boundaries.

(5) An increase in the dislocation density within the grain interior.

(c) The effect of the electric field on cavitation was mainly on the cavities which formed along the grain boundaries (especially at triple points) compared to those which formed at inclusions, Fig. 26.

(d) An increase in the number of whiskers, Fig. 27, which occurred on the fracture surface of specimens which had been superplastically deformed with an electric field compared to without. These whiskers appeared to have resulted from a very large elongation (> 1000%) of the very ductile DFZ.

(e) A decrease in the activation energy for superplastic deformation by the electric field both at lower temperatures (437°C) and at higher temperatures (567°C) than those normally employed (516–520°C) for the superplastic deformation of 7475 Al; see Fig. 28.

The following explanations were proposed for the above experimental results in terms of current theories pertaining to the superplastic deformation of metals:

(a) Strain-Enhanced Grain Growth: The early stage of grain growth in Fig. 23 is in accord with the strain-enhanced grain growth relation proposed by Wilkinson and Caceras [48]

$$\Delta d_\varepsilon = K \dot{\varepsilon}^{-p} \varepsilon \qquad (12)$$

where K and p are constants and $\dot{\varepsilon}$ is the strain rate. The direct observation by us of dynamic recrystallization during the later stage in Fig. 24 provides support for Ghosh and Raj's [49] interpretation of the decrease in grain size with strain they observed during the superplastic deformation of 7475 Al.

The retarding effect of the electric field on initial grain growth is through a reduction in the product $K\,\dot{\varepsilon}^{p}$, which could result from either a reduction in grain boundary mobility *per se* or an increased retarding effect on grain boundary mobility by the larger dispersoids in the DFZ-grain boundary region.

(b) Dispersoid-Free Zone (DFZ): The observed proportionality between the ratio $\bar{S}/\bar{L}$ and strain in Fig. 25 is in accord with the expression derived by Karim et al [50] and Valiev and Kaibyshev [51] for diffusion creep strain

$$\varepsilon_{DC} = \bar{S}/\bar{L} \qquad (13)$$

(c) Cavitation: The linear increase in volume fraction of cavities with the logarithm of the strain is in accord with the expression derived by Hancock [52] for strain-controlled growth of cavities, namely

$$\frac{dr}{d\varepsilon} = \frac{\eta}{3}\left(r - \frac{3\gamma_s}{2\sigma}\right) \qquad (14)$$

where r is the cavity radius, γ_s the specific surface energy, σ the Von Mises stress and η the cavity growth rate parameter. If $3\gamma_s/2\sigma$ is sufficiently small, Eqn. 14 can be rewritten as

$$\frac{dV}{d\varepsilon} = \eta_v V \qquad (15)$$

where V is the total cavity volume and η_v the volume cavity growth rate parameter. Integration of Eqn. 15 gives

$$\ln f_v = K + \eta_v \varepsilon \qquad (16)$$

which is in accord with the observed increase in volume fraction of cavities with strain. The electric field increased both K and η_v, the greater

effect being on K, which is a measure of the number of cavities per unit volume, i.e. the cavity nucleation rate. The slight increase in η_v with electric field reflects an increase in the ease of grain boundary sliding [53,54].

(d) Flow Stress: Steady state superplastic flow can be expressed by [55]

$$\dot{\varepsilon} = \left(\frac{AD\mu b}{kT}\right)\left(\frac{b}{d}\right)^{p}\left(\frac{\sigma}{\mu}\right)^{1/m} \qquad (17)$$

where $\dot{\varepsilon}$ is the strain rate, σ the flow stress, A a dimensionless constant, D the appropriate diffusion coefficient, μ the shear modulus, b the Burgers vector, d the grain size, p the grain size exponent, m the strain rate hardening exponent and kT has its usual meaning. Rearranging Eqn. 17 one obtains for the flow stress

$$\sigma = \left(\frac{kT}{AD\mu b}\right)^{m}\left(\frac{d}{b}\right)^{pm}\mu\dot{\varepsilon}^{m} \qquad (18)$$

An analysis of the change in the stress-strain behavior produced by the electric field suggests that the influence of the field is through its effect on the parameters A and p [43]. It is proposed that the effect on A is through the influence of the field on the microstructure and on p through an increase in the grain boundary sliding and diffusion flow contributions to the plastic deformation rate. The observed increase in the strain rate hardening parameter m and the decrease in the activation energy Q by the field are in accord with this idea. Moreover, the increase in the width of the DFZ suggests that the electric field promotes diffusional plastic flow. This would contribute to the observed increase in m and p with electric field.

The detailed mechanism(s) by which the electric field produces the effects discussed above is not clear. However, all of the effects can be explained in terms

of an increased diffusion rate produced by the electric field, thereby enhancing the diffusion-controlled mechanisms responsible for grain boundary sliding and diffusion creep, and producing the changes in microstructure which occur during the superplastic deformation. Especially affected appears to be grain boundary sliding as evidenced by the significant reduction in cavitation along the boundaries.

The various effects of the electric field can be explained qualitatively by the model illustrated in Fig. 29, which is similar to that proposed for the effect of electric field on quench aging in α-iron in Fig. 14. In this model the charge produced by the field at the specimen surface influences there the chemical potential of vacancies in such a manner as to promote the diffusion of the charged vacancies from the grain interior to the grain boundaries and thence rapidly along the boundaries to the surface. If this model is correct, then the effect of the field would depend on the specimen grain size and its thickness. An estimate of the time required for a vacancy to reach the surface from the interior of a grain at the center of the specimen can be obtained from the diffusion equation

$$x = 2\sqrt{Dt} \qquad (19)$$

and

$$t = t_g + t_{gb} \qquad (20)$$

where x is the diffusion distance, $D = D_0 \exp(-\Delta H/kT)$ the appropriate diffusion coefficient, t_g the time for a vacancy to diffuse from the interior of the grain to the grain boundary and t_{gb} the time to reach the surface along the grain boundary. For the calculation we will assume that the distance x_g from the interior of the grain to the boundary is approximately one half the grain size (~ 5 μm) and the distance x_{gb} along the grain boundaries to the specimen surface is approximately half the specimen thickness (0.6 mm). The coefficient for the lattice diffusion of

vacancies in Al is $D_l^v = 0.2 \exp(-11{,}500/RT)$ [56,57]; that for diffusion of vacancies along grain boundaries is not known, but the activation energy for grain boundary diffusion of vacancies is estimated to be 1/4 to 1/2 that for diffusion in the lattice [58,59]. Hence, it will be assumed here that the diffusion coefficient for vacancies along the grain boundaries $D_g^v = 0.2 \exp(-5{,}750/RT)$. Taking the above values and T = 516°C (typical superplastic deformation temperature for 7475 Al), one obtains using Eqns. 19 and 20, t ≈ 0.2s, which is well within the response time noted on recordings of changes in the stress-strain curves when the field was turned on and off [44]. Thus, the estimated time for the operation of the proposed model is well within that which would be required for the superplastic deformation of the 7475 Al alloy sheet of 1.2 – 1.8 mm thickness and 8–10 μm initial grain size.

Assuming the above model for the effect of an external electric field on the superplastic deformation of 7475 Al and taking the vacancy diffusion coefficient $D_g^v = 0.2 \exp(-5{,}750/RT)$, one obtains 2.9 mm as the limiting specimen thickness for the test conditions T = 516°C, t = 1s, and grain size d = 10 μm. This limiting thickness is considered to be a lower bound value, since the activation energy for the diffusion of vacancies along a large angle grain boundary is expected to be less than 1/2 that for their diffusion in the lattice [59].

3. SUMMARY AND CONCLUSIONS

The studies during this report period confirm and extend the earlier findings by the author and his coworkers [1] that an internal electric current or an external electric field can have an influence on the mechanical properties of metals and on solid state transformations therein in addition to the usual side effects of Joule heating, etc. Significant effects occurred for electric currents ≥ ~

kA/cm^2 (continuous d.c. or a.c. and pulsed d.c.) and for continuous d.c. electric fields > ~ kV/cm. They were attributed mainly to an influence on the mobility of crystal defects. The effects which were observed include the following:

(a) Electric Current

(1) **Quench Aging of a Low-Carbon Steel**: A continuous d.c. current of ~ 1 kA/cm^2 enhanced the rate of quench aging at 80°C, whereas a continuous a.c. of ~ 100 Hz retarded the rate very significantly. The frequency of 100 Hz is approximately that for the jump frequency of C atoms at the aging temperature. However, an explanation for the influence of the current on the aging rate is not straightforward, because the diffusion of C atoms, C atom-vacancy complexes and individual vacancies are involved in the nucleation and growth of at least two precipitate forms. A complex effect of a.c. and d.c. current on aging has also been reported by others for Al-Cu and Al-Zn alloys.

(2) **Mechanical Properties**: High density, d.c. electric current pulses (≥ kA/cm^2 for 100 μs) increased the plastic deformation rate by orders of magnitude at low and intermediate homologous temperatures ($T < \sim 0.3\ T_M$) as a result of an increase in the mobility of dislocations. The increased mobility resulted from an effect of the drift electrons on several of the parameters in the thermally activated rate equation, the major effect being on the pre-exponential.

An increase in fatigue life of polycrystalline Cu resulted when high density electric current pulses were continuously applied during cycling at constant stress. The prolonged life is attributed to the increased homogenization of slip which occurred. This was considered to result from the increased dislocation mobility produced

by the current pulses. An increased dislocation mobility was also concluded to be responsible for the elimination of the cyclic hardening by electropulsing during the low cycle fatigue of α-Ti.

(3) **Recovery, Recrystallization and Grain Growth**: High density electric current pulses enhanced the rates of recovery and recrystallization, but retarded the rate of grain growth at temperatures just above the recrystallization temperature. The enhancement of the rates of recovery and recrystallization is considered to result from an increase in dislocation mobility and of vacancy migration rate. The retardation of grain growth was deduced to result from a reduction in the residual dislocation density in the recrystallized grains due to the increased dislocation mobility during recrystallization produced by the drift electrons.

(b) Continuous d.c. Electric Field

(1) **Quench Aging of a Low-Carbon Steel**: An external electric field of ~ 14 kV/cm retarded the rate of age hardening and reduced the peak hardness. TEM observations revealed that associated with these effects there occurred an appreciable increase in the width and nature of the relatively precipitate-free zone adjacent to the grain boundaries. It was therefore concluded that the effects of the field were mainly due to the enhanced migration of the quenched-in vacancies from the grain interior to the grain boundary and thence to the external surface as a result of the electric charge produced at the surface by the field. Again, the details of the effect of the field on the aging process are complex, because C atoms, C atom-vacancy complexes and individual vacancies are involved in the nucleation and growth of at least two precipitate forms.

(2) **Hardenability of Steel**: The application of an electric field of ~ 1 kV/cm during the quenching of a tool steel increased the hardenability as measured by a simulated Jominy end-quench test by shifting the CT curve to longer times. The present tests did not establish which of the various parameters that govern the rate of pearlite growth was influenced by the field. However, a major affect may be on the diffusion of C along the grain boundaries during the formation of pearlite.

(3) **Annealing of Ni_3Al**: An electric field of ~ 2 kV/cm retarded the rates of recovery and recrystallization of Al and Cu, but enhanced them in Ni_3Al. The retardation in Al and Cu is considered to result from the removal of vacancies from the specimen interior to the surface. The results on Ni_3Al thus suggest that either recovery and recrystallization in this material are enhanced by a reduction in vacancy concentration or that the influence of the electric field is by a different mechanism.

(4) **Superplasticity of 7475 Al**: The application of an electric field of ~ 1 kV/cm during the superplastic deformation of 7475 Al produced the following effects: (a) reduced the flow stress, (b) increased the strain rate hardening exponent, (c) retarded grain growth, (d) increased the width of the dispersoid-free zone and changed its chemistry, (e) increased the dislocation density and size of the dispersoids within the grains and (f) reduced cavitation. These effects were all attributed to an increased diffusion of vacancies resulting from the charge at the external surface produced by the electric field.

As an overall summary of the results obtained to-date: High density d.c. electric current ($\geq$ kA/cm^2) enhances dislocation mobility at all temperatures and

atomic or vacancy diffusion at elevated temperatures. a.c. current of the proper frequency can significantly retard diffusion-controlled processes. The application of an electric field can influence superplastic deformation or other diffusion-controlled processes by affecting the diffusion of vacancies as a result of the electric charge produced by the field at the external surface. Thus, electric currents and fields offer the possibility of either enhancing or retarding (and perhaps even completely suppressing) metal phenomena, thereby providing potential for improving the efficiency of processing operations and/or improving the properties of the product.

4. ACKNOWLEDGEMENTS (Participating Personnel)

The author acknowledges the assistance of Dr. A. F. Sprecher, senior research associate, in carrying out all phases of this research program. He also wishes to acknowledge the following persons who contributed to various aspects of the work:

Post Doctoral Fellows	Visiting Scholars	Graduate Students
Dr. H. A. Lu	Ms. X. P. Lu	W. D. Cao, Ph.D. 1989
Dr. W. D. Cao	Mr. Z. Guo	J. Campbell, M.S. expected 1993
Dr. Y. Chen	Prof. M. Zheng	J. Barnak
		M. Fisher
		K. Wade

5. REFERENCES

1. H. Conrad, "A Study Into the Mechanism(s) for the Electroplastic Effect in Metals and Its Application to Metalworking, Processing and Fatigue", U.S. ARO Funding Document DAAL03–86–K–0015, March 10, 1989.
2. Erdmann-Jesnitzer, D. Mrowka and K. Ouvier, Arch. für Eisenhüttenwesen **30** (1959) 31.
3. F. Erdmann-Jesnitzer and K. Ouvier, Vortragen XI Berg-und Huttenmännischen Tag der Bergakademie Freiberg, (21–23 May 1959), Freiberger forschungshafte B **50** (1960) 136.
4. T. J. Koppenaal and C. R. Simcoe, Trans. TMS-AIME **227** (1963) 615.
5. M. C. Shine and S. R. Herd, Appl. Phys. Lett. **20** (1972) 217.
6. Y. Onodera and K. Hirano, J. Mat. Sci. **11** (1976) 809.
7. Y. Onodera, J. Maruyama and K. Hirano, J. Mat. Sci. **12** (1977) 1109.
8. Y. Onodera and K. Hirano, J. Mat. Sci. **19** (1984) 3935.
9. C. Wert, in **Thermodynamics in Physical Metallurgy**, ASM, Metals Park, OH (1950) p. 178.
10. W. C. Leslie, Acta Metallorg. **9** (1961) 1004.
11. A. S. Keh and Leslie, in **Structure and Properties of Engineering Materials**, Mat. Sci. Res. Vol. 1, ed. by H. H. Stadelmaier and W. W. Austin, Plenum Press, New York, NY (1963) p. 208.
12. James Campbell and Hans Conrad, "The Effects of d.c. and a.c. Current on the Quench Aging of a Low Carbon Steel", in preparation for publication.
13. H. Conrad, Y. Chen and A. F. Sprecher, "The Influence of an Electric Charge on the Quench Aging of a Low Carbon Steel", in TMS-ASM **Int. Symp. Microstructures and Mechanical Properties of Aging Materials**, Chicago, IL, Nov. 4, 1992, in print.

14. T. Okabe and A. G. Guy, Met. Trans. **1** (1970) 2705.

15. R. A. Johnson, **Diffusion in BCC Metals**, ASM, Metals Park, OH (1965) p. 155.

16. M. Kiritani, H. Takata, K. Moriyama and F. E. Fujita, Phil. Mag. **A40** (1979) 779.

17. Wei-di Cao, A. F. Sprecher and H. Conrad, J. Phys. E.: Sci. Instrum **22** (1989) 1026.

18. Wei-di Cao, A. F. Sprecher and H. Conrad, in **High Temperature Niobium Alloys**, ed. by J. J. Stevens and I. Ahmad, TMS, Warrendale, PA (1991) p. 27.

19. H. Conrad, W. D. Cao and A. F. Sprecher, in **Constitutive Laws of Plastic Deformation and Fracture**, Kluwer Academic, Netherlands (1990) p. 305.

20. H. Conrad, A. F. Sprecher, W. D. Cao and X .P. Lu, JOM **42** (1990) 28.

21. V. Ya Kravchenko, Zh. Eksp. and Theor. Fiz. 51 (1966) 1676; Sov. Phys.-JETP **24** (1967) 11135.

22. M. I. Kaganov, V. Ya Kravchenko and V. D. Natsik, Usp. Fiz. Nauk **111** (1973) 655; Sov. Phys.-Usp. **16** (1974) 878.

23. K. M. Nimov, G. O. Shnyrev and I. I. Novikov, Dokl. Acad. Nauk SSSR **219** (1974) 323; Sov. Phys.-Dokl. **19** (1975) 787.

24. F R. N. Nabarro, Theory of Dislocations (Oxford: Carendon Press, 1967) p. 529. Reprinted 1987 (New York: Dover).

25. A. M. Roshchupkin, V. E. Miloshenko and V. E. Kalinin, Fiz. Tverd. Tela **21** (1978) 90; Sov. Phys.-Solid State 21 (1979) 532.

26. V. B. Fiks, Zh. Eksp. Theor. Fiz. **80** (1981) 2313.

27. H. Conrad and A. F. Sprecher, in **Dislocations in Solids**, Chap. 43, ed. by F. R. N. Nabarro, Elsevier Sci., B. V. (1989) p. 497.

28. H. Conrad, J. White, W. D. Cao, X. P. Lu and A. F. Sprecher, Mat. Sci. Engr. **A145** (1991) 1.

29. Wei-di Cao and Hans Conrad, Fatigue Fract. Engr. Mater. Struct. **15** (1992) 573.

30. Z. H. Lai, C. X. Ma and H. Conrad, Scripta Met. Mat. **27** (1992) 527.

31. H. Conrad, Z. Guo, M. Fisher, W. D. Cao and A. F. Sprecher, in **Recrystallization '90**, ed. by T. Chandra, TMS, Warrendale, PA (1990) p. 301.

32. H. Conrad, Z. Guo and A. F. Sprecher, Scripta Met. and Mat. **24** (1990) 359.

33. J. C. M. Li, in **Recrystallization, Grain Growth and Textures**, ed. by H. Margolin, ASM, Metals Park, OH (1966) p. 45.

34. K. Lücke and H.-P. Stüwe, in **Recovery and Recrystallization of Metals**, ed. by L. Himmel, Gordon and Breach, N. Y. (1963) p. 171.

35. H. Lu and H. Conrad, Appl. Phys. Lett. **59** (1991) 1847.

36. H. Conrad, Y. Chen and H. Lu, in TMS-ASM **Int. Symp. Microstructures and Mechanical Properties of Aging Materials**, (Nov. 4, 1992, Chicago) in print.

37. W. D. Cao, X. P. Lu, A. F. Sprecher and H. Conrad, Mater. Lett. **9** (1990) 193.

38. M. Zheng and H. Conrad, "Influence of an Electric Field on the Cooling-Transformation Curves for a Tool Steel", in preparation for publication.

39. H. E. Boyer and J. J. Kubbs (eds.), Heat Treaters Guide, ASM P. M. Unterweiser, Metals park (1982) p. 264–265.

40. J. W. Cahn and W. C. Hagel, in **Decomposition of Austenite in Diffusional Processes**, ed. by V. F. Zackay and H. I. Haronson, Interscience, N. Y. (1962) p. 131.

41. J. D. Verhoeven, **Fundamentals of Physical Metallurgy**, Wiley, N. Y. (1975) p. 428–444.

42. H. Conrad, Z. Guo and A. F. Sprecher, Scripta Metall. **23** (1989) 821.

43. W. D. Cao, X. P. Lu, A. F. Sprecher and H. Conrad, Mat. Sci. Engr. **A129** (1990) 157.

44. W. D. Cao, X. P. Lu, A. F. Sprecher and H. Conrad, in **Superplasticity in Aerospace II**, ed. by T. r. McNelley and H. C. Heikkenen (1990) p. 269.
45. H. Conrad, W. D. Cao, X. P. Lu and A. F. Sprecher, Mat. Sci. Engr. **A138** (1991) 247.
46. X. P. Lu, W. D. Cao, A. F. Sprecher and H. Conrad, J. Mat. Sci. **27** (1992) p. 2243.
47. M. K. Rao and A. K. Mukherjee, Mat. Sci. Engr. **80** (1986) 181.
48. D. S. Wilkinson and C. H. Ceceres, Acta Metall. **32** (1984) 1335.
49. A. K. Ghosh and R. Raj, in **Superplasticity** ed. by B. Baudelat and M. Surey, Editions du CNRS, Paris (1985) p. 11.1.
50. A.-V.L. Karim, D. L. Holt and W. A. Backofen, Trans. AIME **245** (1969) 2421.
51. R. Z. Valiev and O. A. Kaibyshev, Acta Metall. **12** (1983) 2121.
52. J. W. Hancock, Mat. Sci. **10** (1976) 319.
53. M. Surey in **Superplasticity**, ed. by B. Baudelet and M. Surey, Editions de CNRS, Paris (1985) p. 8.1.
54. B. Budiansky, J. W. Hutchinson and B. Slutsky, in **Mechanics of Solids**, ed. by H. G. Hopkins and M. J. Stowell, Pergamon, Oxford (1982) p. 13.
55. A. K. Mukherjee, J. E. Bird and J. E. Dorn, Trans. ASM **62** (1969) 155.
56. P. G. Shewmon, **Diffusion in Solids**, McGraw-Hill, N. Y. (1963) p. 74.
57. R. A. Johnson, in **Diffusion**, ASM, Metals Park, OH (1973) p. 25.
58. N. A. Gjostein, in **Diffusion**, ASM, Metals Park, OH (1973) p. 241.
59. N. Nomura, S.-Y. Lee and J. B. Adams, J. Mater. Res. **6** (1991) 1.

TABLE 1. Data pertaining to self-diffusion and C-diffusion in a-Fe.

Self-diffusion in α-Fe

Bulk Diffusion				Grain Boundary Diffusion			
D_o (cm^2/s)	Q_f^v (eV)	Q_m^v (eV)	Q_D (eV)	D_o (cm^2/s)	Q_f^v (eV)	Q_m^v (eV)	Q_D (eV)
0.5(1)	1.3+0.4(2)	0.68(3)	2.62(1)	0.2(6)	—	—	1.57(6)
118(4)	—	1.24+0.14(5)	2.92(4)	—	1.2(7)	0.2(7)	
18(4)	—	—	2.78(4)	1.7(4)	—	—	1.74(4)

C diffusion in α-Fe

D_o^C (cm^2/s)	Q_m^C (eV)	Q_m^{C-v} (eV)	Q_B^{C-v} (eV)
0.008(8)	0.86(8)	0.43(2)	0.41(2)
0.004(9)	0.83(9)	0.41(10)	0.41(3)
0.026(10)	0.89(10)		0.41(11)
	0.86(11)		0.40(12)
	0.87±0.07(12)		
4.0(12)	0.833(12)		
0.02(4,13)	0.87(4,13)		

Notes:

Numbers in parenthesis are references given below.
D_o, Q_f^v, Q_m^v and Q_D are the pre-exponential and the energies respectively for vacancy formation, vacancy migration and self-diffusion in α-Fe.
D_o^C, Q_m^C, Q_m^{C-v} and Q_B^{C-v} are the pre-exponential and the energies respectively for single C atoms diffusion, C-vacancy complex migration and C-vacancy binding.

References

1. D. Lazarus, **Diffusion in BCC Metals**, ASM (1965) p. 155.
2. G. G. Homan, ibid, p. 77.
3. R. A. Johnson, ibid, p. 357.
4. P. G. Shewmon, **Diffusion in Solids**, McGraw-Hill (1963) p. 66 and p. 171.
5. M. Kiritani, H. Takata, K. Moriyama and F. E. Fujita, Phil. Mag. A **40** (1979) 779–802.
6. N. A. Gjostein, **Diffusion**, ASM (1973) p. 241.
7. Estimated from results for Cu by M. Nomura, S-Y Lee and J. B. Adams, J. Mater. Res. **6** (1991) 1.
8. C. A. Wert, Phys. Rev. **76** (1949) 1169.
9. A. E. Lord and D. N. Beshers, reported by R. Gibala and C. A. Wert in **Diffusion in BCC Metals**, ASM (1965) p. 135.
10. R. Gibala and C. A. Wert, **Diffusion in BCC Metals**, ASM (1965) p. 131.
11. A. C. Damask, ibid, p. 317.
12. D. N. Beshers, **Diffusion**, ASM (1973) p. 209.
13. H. W. Paxton, **Precipitation from Solid Solution**, ASM (1959) p. 208.

TABLE 2. Pre-exponential D_o, activation energy ΔH and mean time of stay τ at 80°C for the diffusion of C in α-iron

Ref.	D_o (cm^2/s)	ΔH kcal/mole	τ(80°C)* 10^{-3}s	$1/\tau$ (80°C) (s^{-1})
1	0.008	19.82	7.98	125
2	0.0041	19.20	5.96	168
3	0.026	20.40	6.57	152
4	0.020	20.10	4.75	210

*$\tau = a_o^2/[24\ D_o \exp(-\Delta H/RT)]$, where $a_o = 2.861$ Å

References

1. C. A. Wert, Phys. Rev. 76 1169 (1949).
2. A. E. Lord and D. N. Beshers, reported by R. Gibala and C. A. Wert in Diffusion in BCC Metals, ASM (1965) p. 135.
3. R. Gibala and C. A. Wert, in Diffusion in BCC Metals, ASM (1965) p. 131.
4. H. W. Paxton, Precipitation from Solid Solution, ASM (1959) 208. This paper refers to Ref. 1 above and to J. K. Stanley, Trans. ASME 185 752 (1949).

TABLE 3. Contributions to the Electroplastic Effect†

Metal	Temp.(K)	σ^* (MPa)‡	$\dot{\varepsilon}_j/\dot{\varepsilon}$	$\dot{\varepsilon}_{0,j}/\dot{\varepsilon}_0$	$\exp\frac{-(\Delta U_j^*-\Delta U^*)}{kT}$	$\exp\frac{(A_j^*-A^*)b\tau^*}{kT}$	$\exp\frac{A_j^* F_{ew}}{kT}$	$\exp\frac{-(\Delta H_j^*-\Delta H^*)}{kT}$
Al	300	9.5	8.8×10^3	5.7×10^3	1.94	0.54	1.48	1.55
Cu	300	27.0	5.8×10^3	2.8×10^3	2.60	0.69	1.17	2.10
Ag	300	26.5	5.0×10^3	1.3×10^3	3.13	0.53	1.21	2.01
Nb	300	42.0	12.0×10^3	2.0×10^3	898	0.0052	1.34	6.03
Al	78	27	26.9×10^3	4.8×10^3	11.65	0.47	1.03	5.64
Cu	78	40	29.1×10^3	1.7×10^3	42.13	0.36	1.14	17.29
Ag	78	39	25.1×10^3	1.7×10^3	44.29	0.28	1.20	14.88
Nb	78	584	66.0×10^3	2.1×10^3	29×10^{10}	1.03×10^{-10}	1.06	31.66

† Calculations based on $j = 5.5 \times 10^5$ A/cm^2 for fcc metals and $j = 4.2 \times 10^5$ A/cm^2 for bcc niobium.

‡ σ^* for fcc metals at $\varepsilon_p = 0.8\%$ and $\varepsilon_{j=0} = 1.67 \times 10^{-4}$ s^{-1}; for bcc niobium at $\varepsilon_p = 2\%$ and $\varepsilon_{j=0} = 1.67 \times 10^{-5}$ s^{-1}.

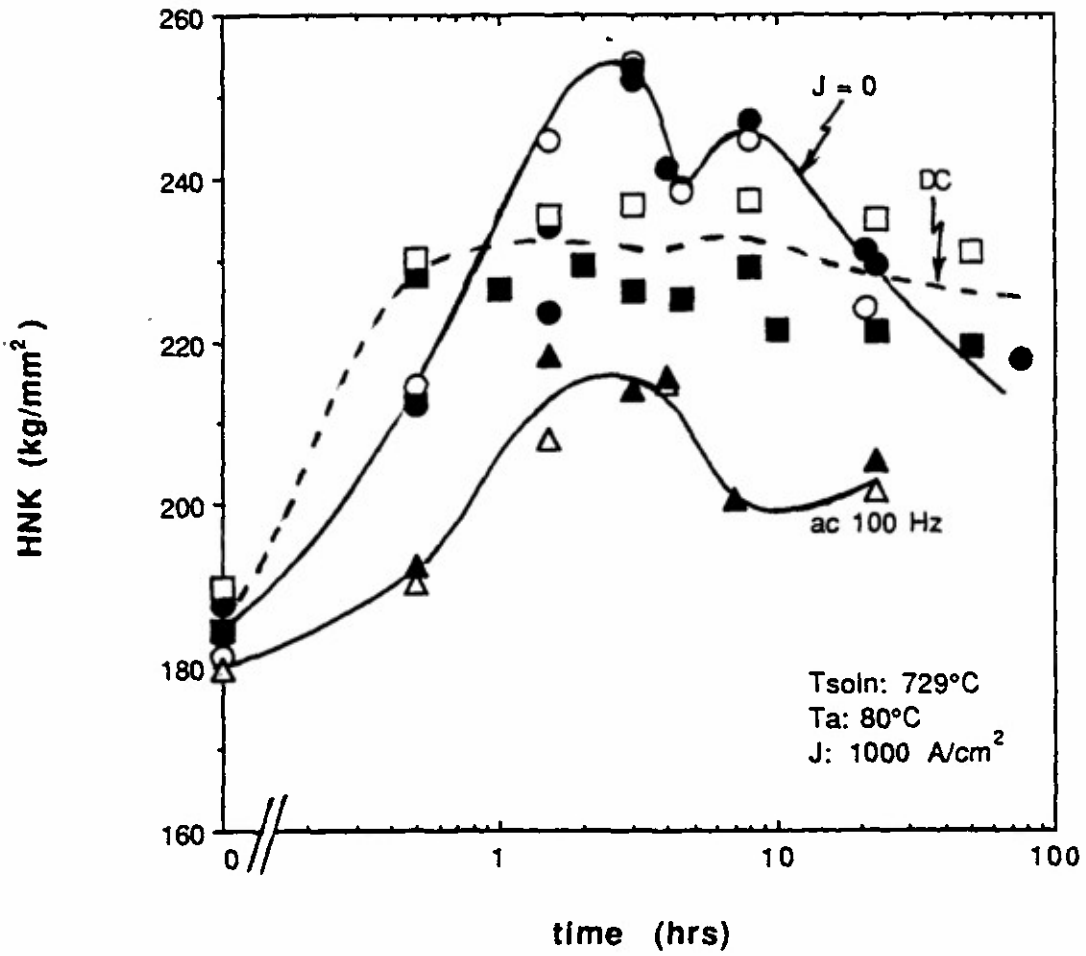

Fig. 1 Effects of d.c. and 100 Hz a.c. on the quench aging (Knoop hardness) of a low-carbon steel at 80°C. Data points are for either 2 or 3 separate specimens.

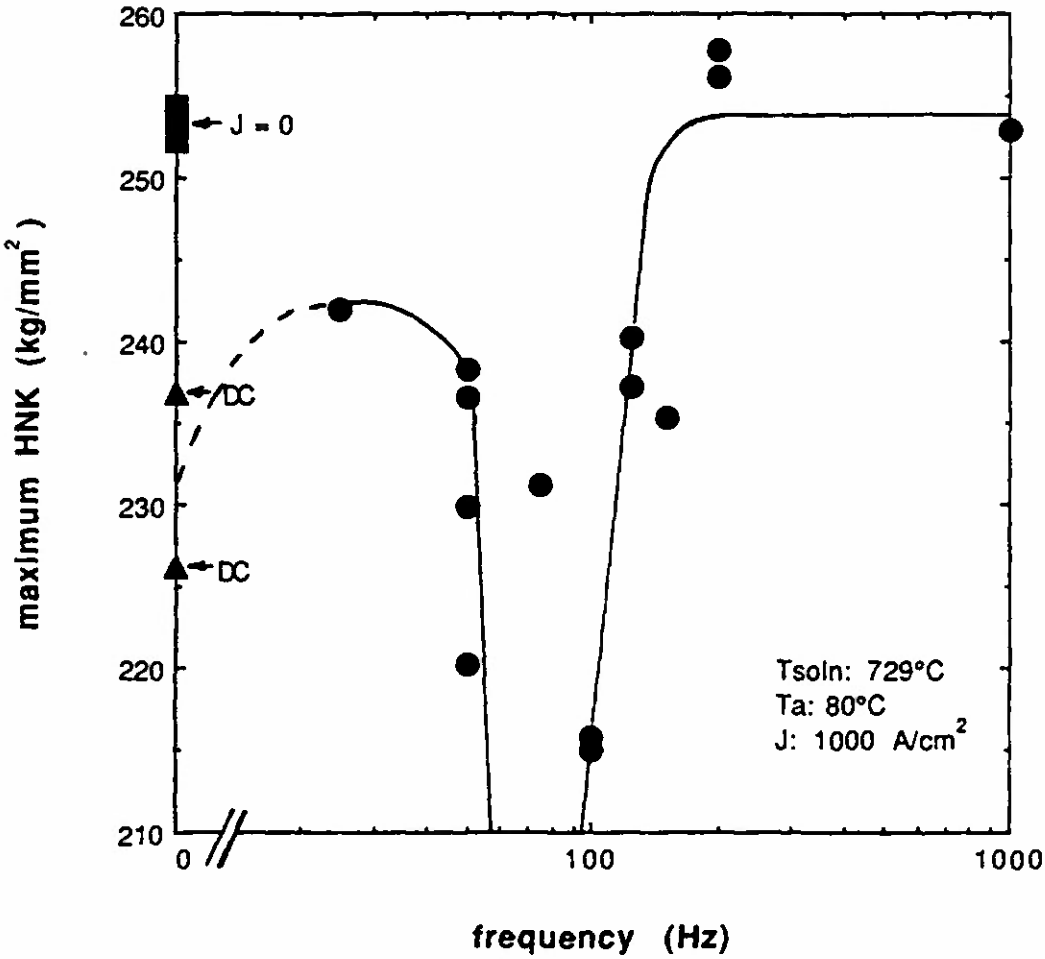

Fig. 2 Effects of d.c. and frequency of a.c. on maximum Knoop hardness for the quench aging of a low-carbon steel at 80°C.

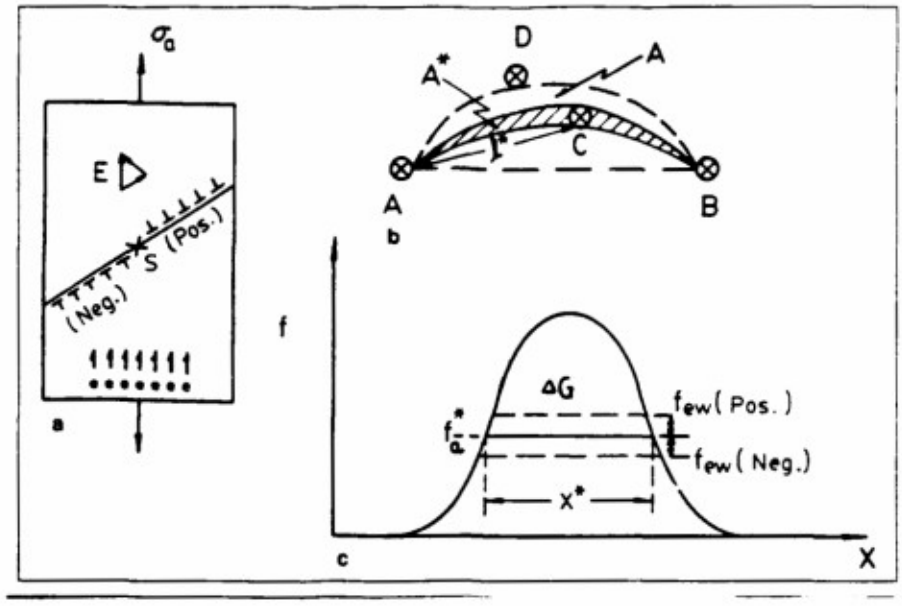

Fig. 3 Schematic of the effect of drift electron flow on dislocation velocity. (a) Specimen subjected to the combined action of a mechanical stress (σ_a) and an electric current (e), with dislocations moving on the glide plane with a velocity parallel (pos.) and antiparallel (neg.) to e. (b) Dislocation segment of length 2l overcomes obstacle (C) by combined action of total applied force and thermal fluctuations. (c) Force-distance curve for overcoming the obstacle (C). $\Delta G = \Delta H^* - T\Delta S^*$ is the Gibbs free energy of activation. $f_a^* = \tau_a^* bl^*$, $f_{ew} = F_{ew} l^*$, x^* = activation distance, $A^* = l^* x^*$ is the activation area, $\tau_a = (\sigma_a - \sigma_i)/M$, where σ_i is the long-range internal stress and M is the Taylor orientation factor.

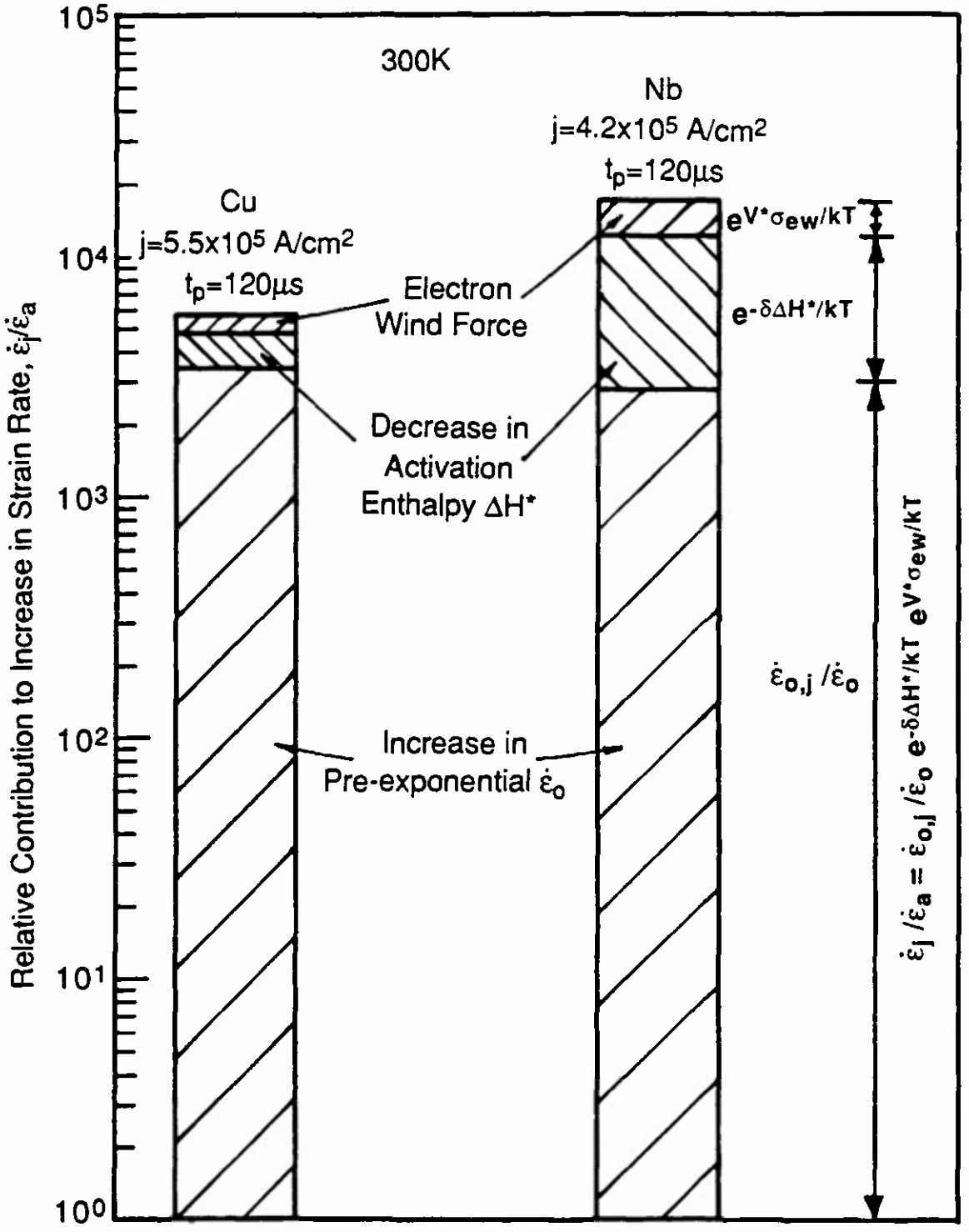

Fig. 4 Relative contributions of the components of the thermally activated rate equation to the electroplastic effect in FCC Cu and BCC Nb.

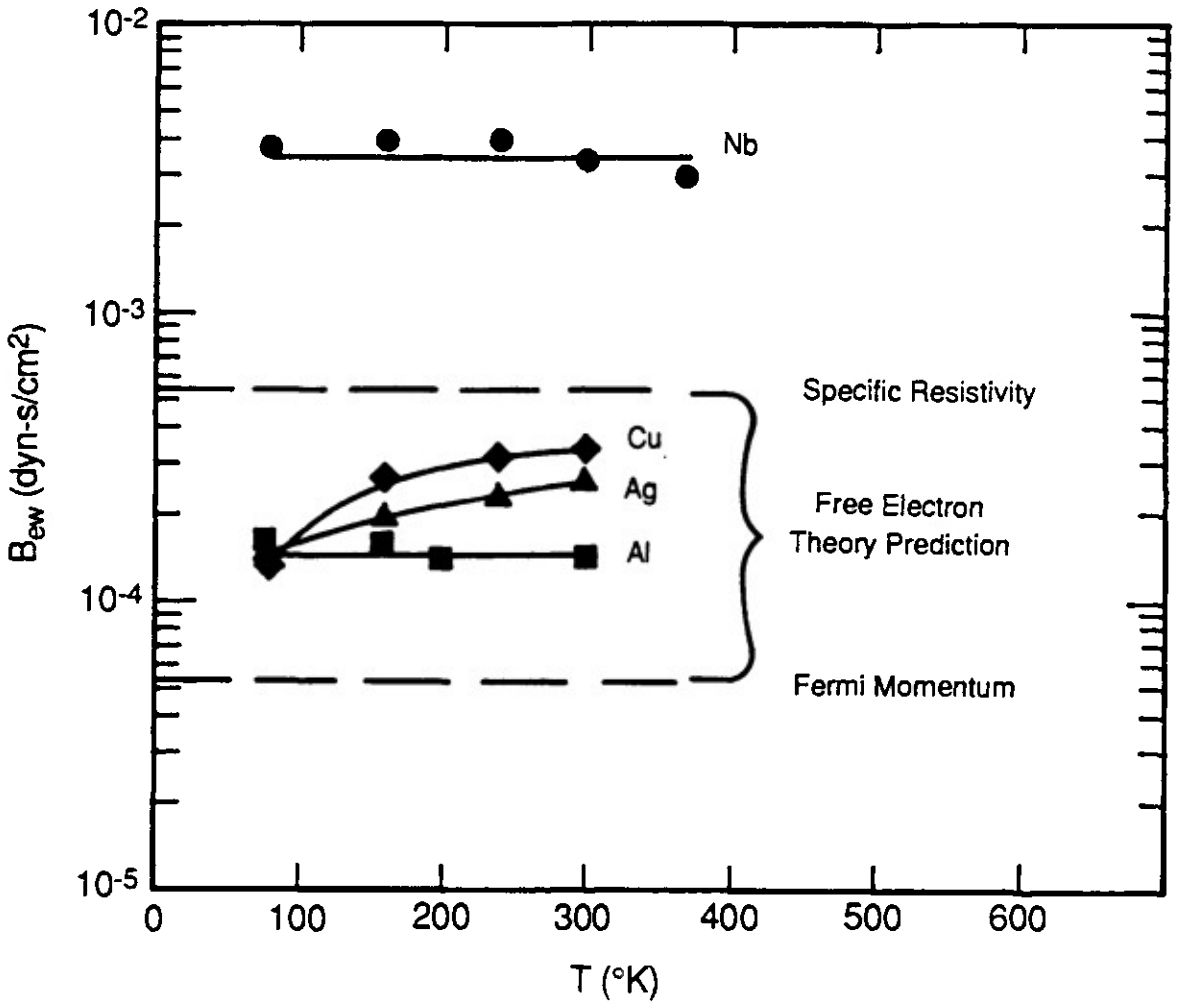

Fig. 5 Comparison of experimentally-derived values of the electron push coefficient B_{ew} with theoretical predictions based on specific dislocation resistivity and Fermi momentum.

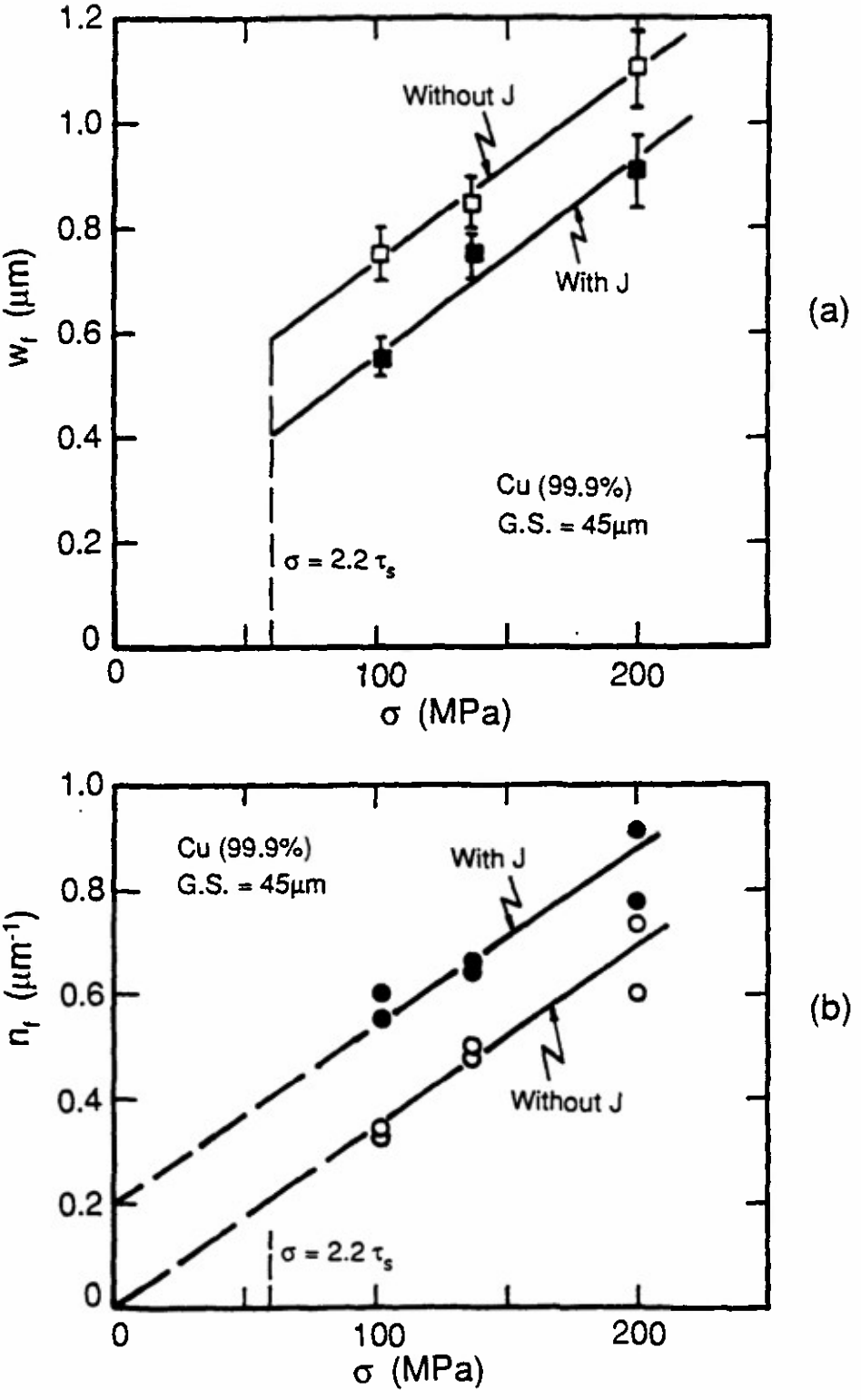

Fig. 6 Effect of electropulsing on the character of persistent slip bands at fracture as a function of cyclic fatigue stress: (a) width and (b) linear density. $\tau_s \approx 28$ MPa is the plateau resolved shear stress (stage B) in the fatigue of Cu single crystals. The factor 2.2 is the Sachs orientation factor.

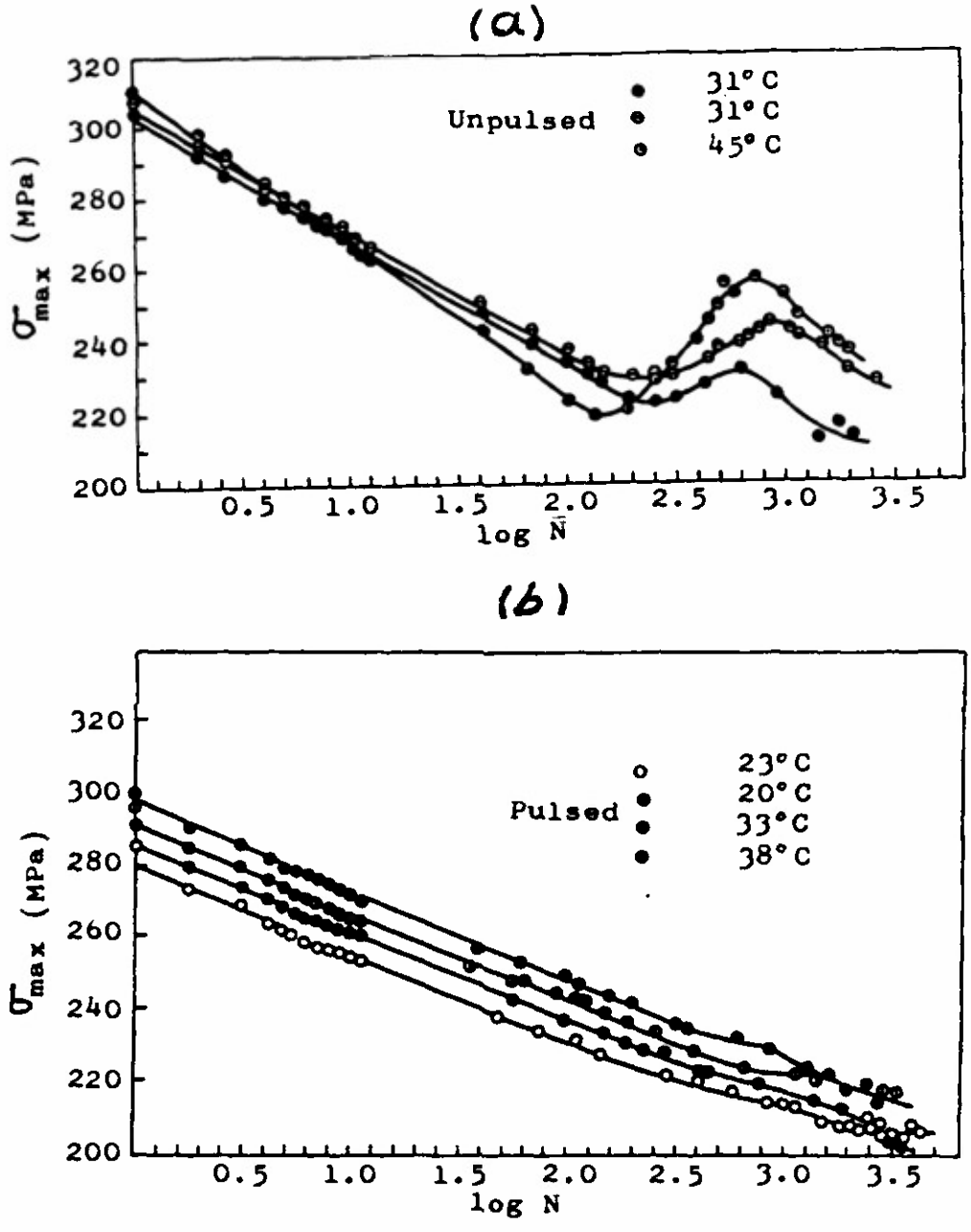

Fig. 7 Effect of electropulsing on cyclic softening and hardening of α-Ti. (a) Not pulsed and (b) pulsed (~ 10^5 A/cm^2, 50 μs duration, 20 pulses per s). From Lai et al [30].

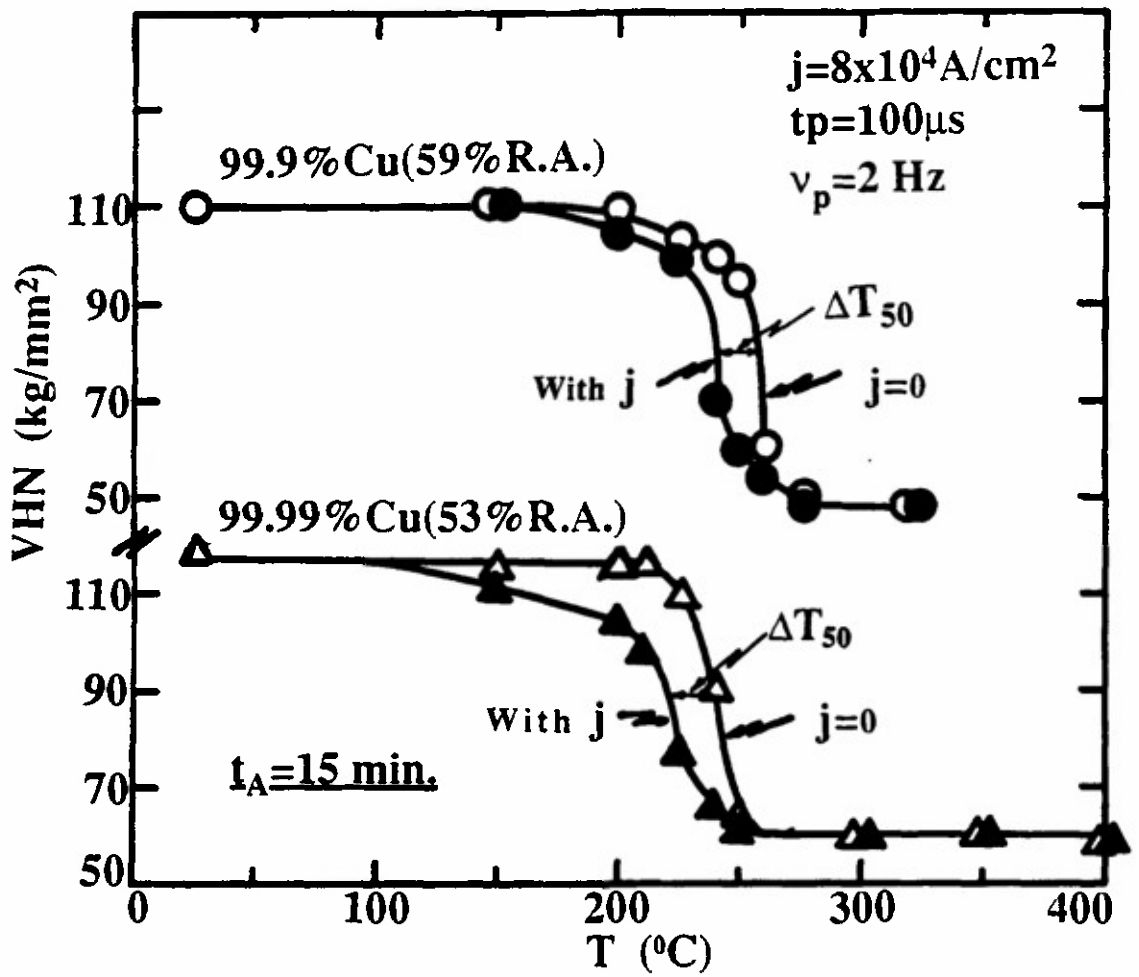

Fig. 8a Effect of electropulsing on the isochronal (15 min) annealing of Cu.

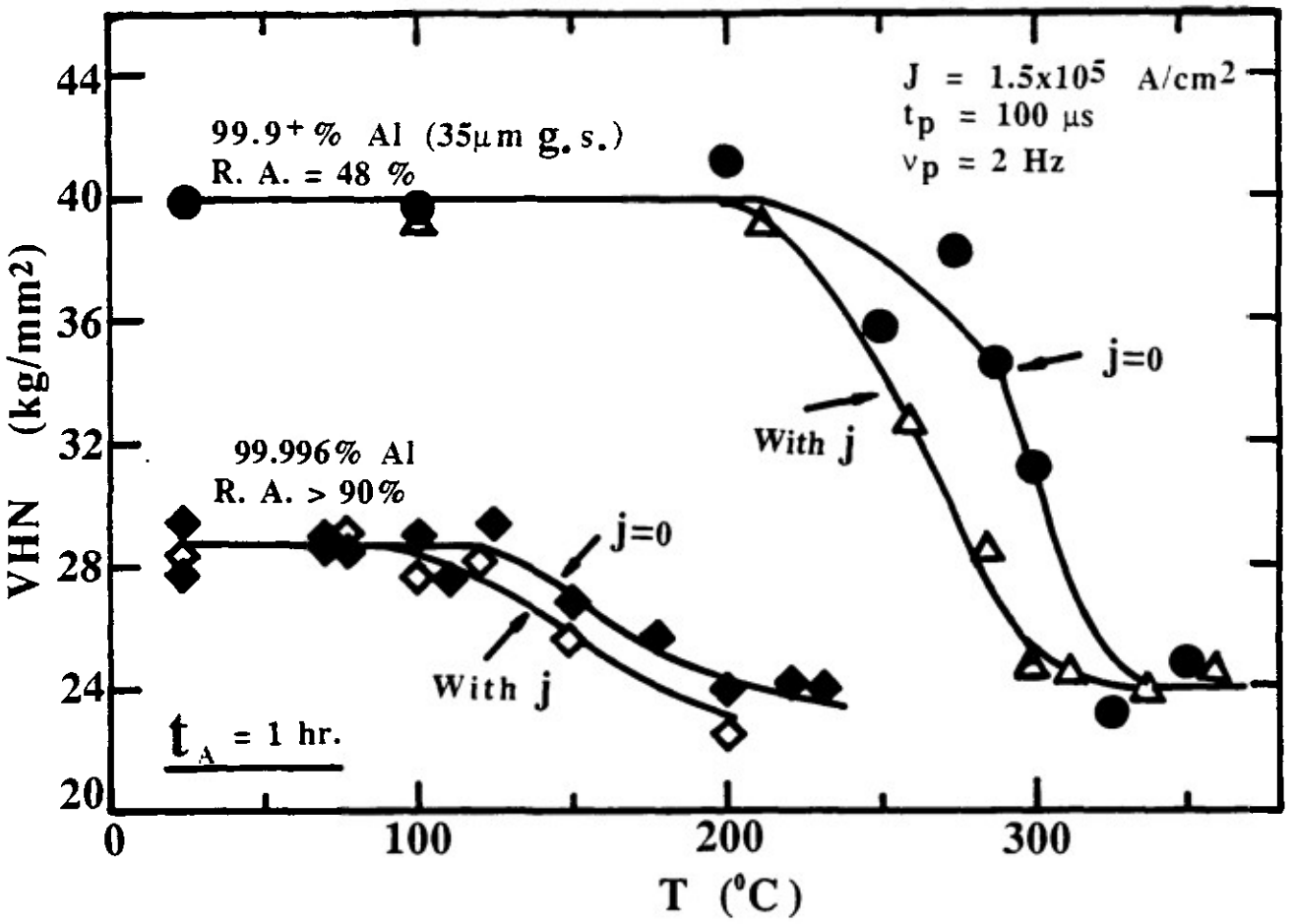

Fig. 8b Effect of electropulsing on the isochronal (1 hr) annealing of Al.

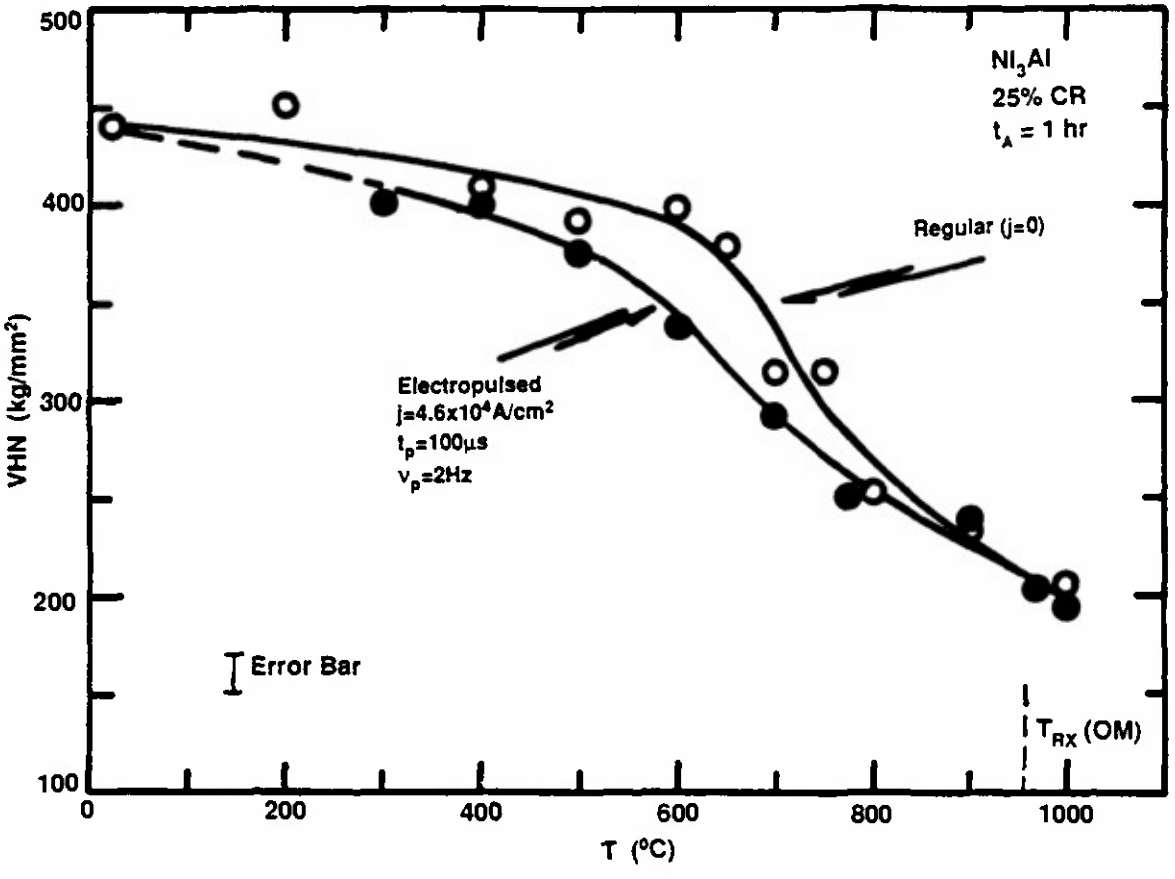

Fig. 8c Effect of electropulsing on the isochronal (1 hr) annealing of Ni_3Al.

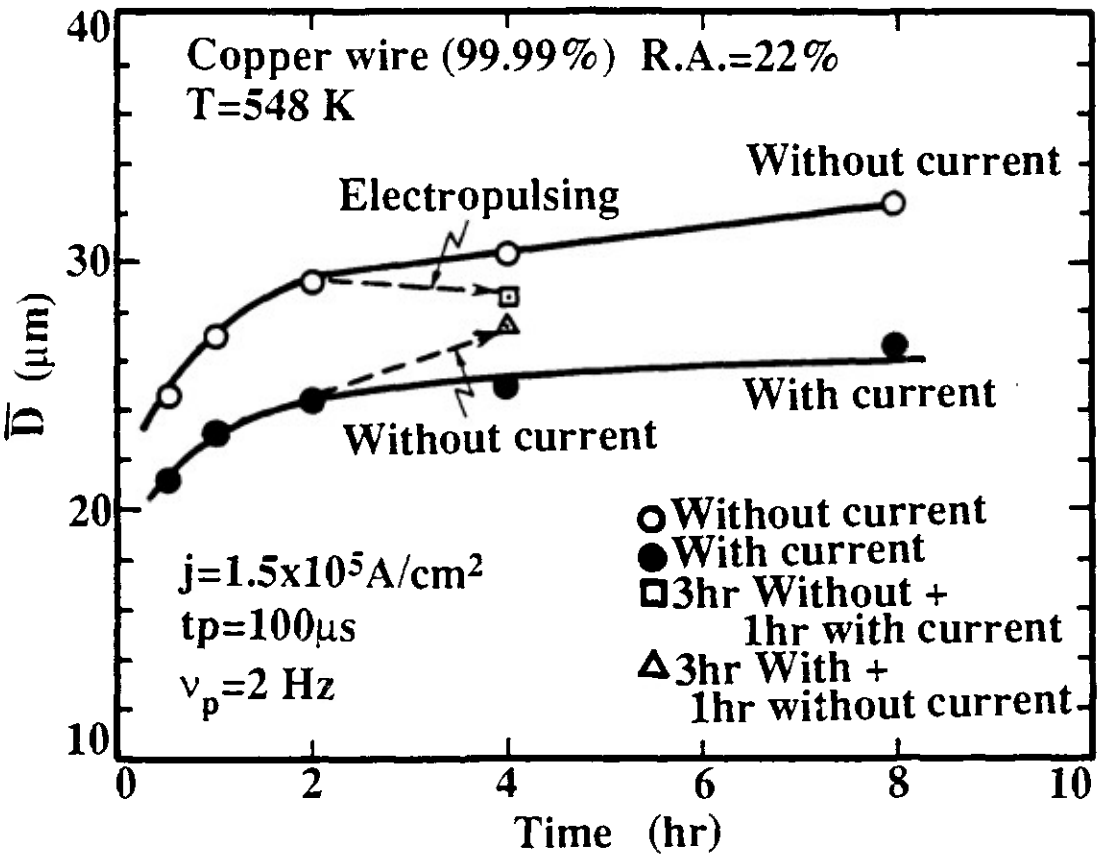

Fig. 9 Effect of electropulsing on grain growth in 99.99 Cu.

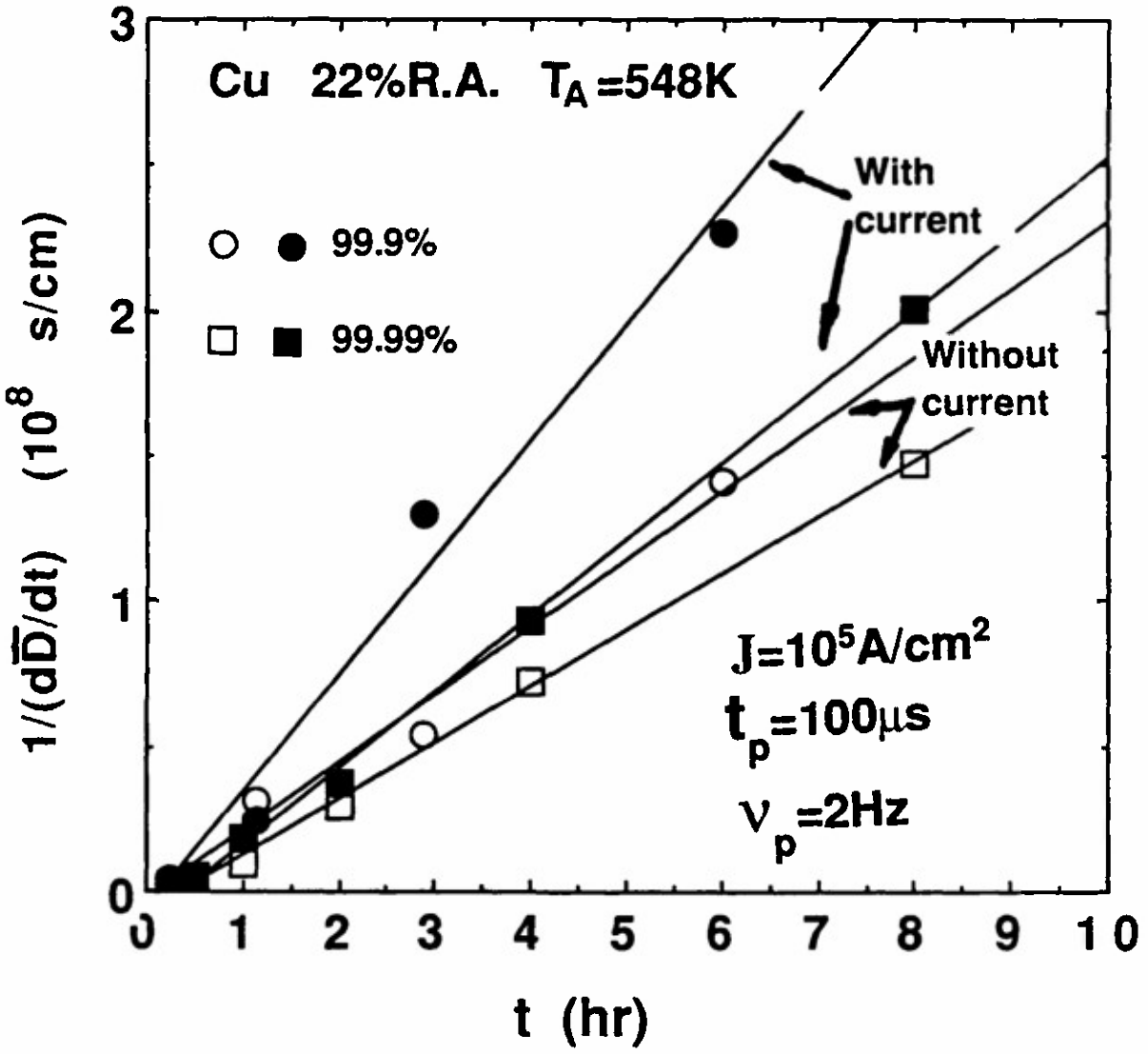

Fig. 10 Effect of electropulsing on the reciprocal of the grain growth rate vs the annealing time for Cu of two purity levels.

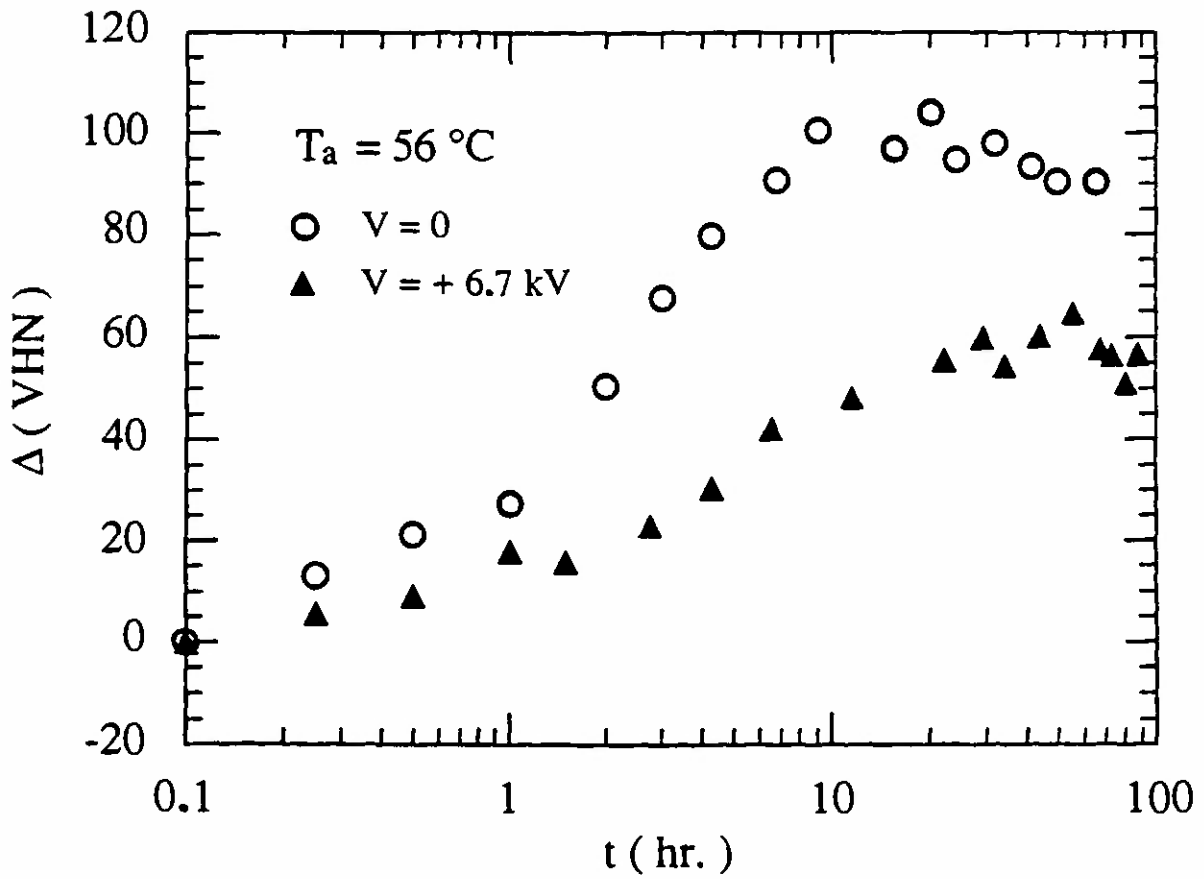

Fig. 11 Effect of applied voltage (external electric field) on the aging curve (increase in Vickers hardness) at 56°C. d = 13 μm.

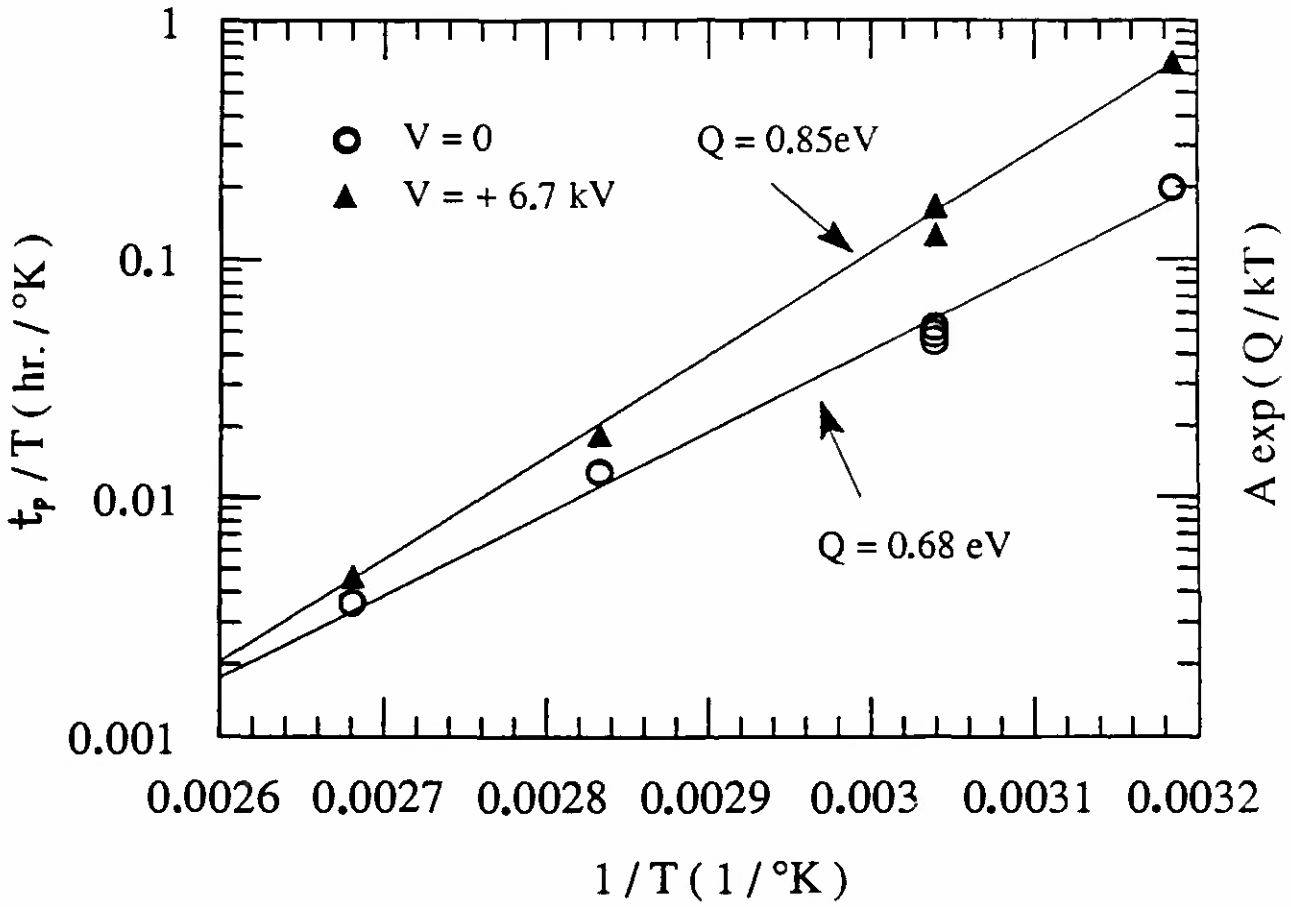

Fig. 12 Semi-log plot of the time to reach maximum Vickers hardness divided by the aging temperature vs reciprocal of the temperature. d = 13 μm.

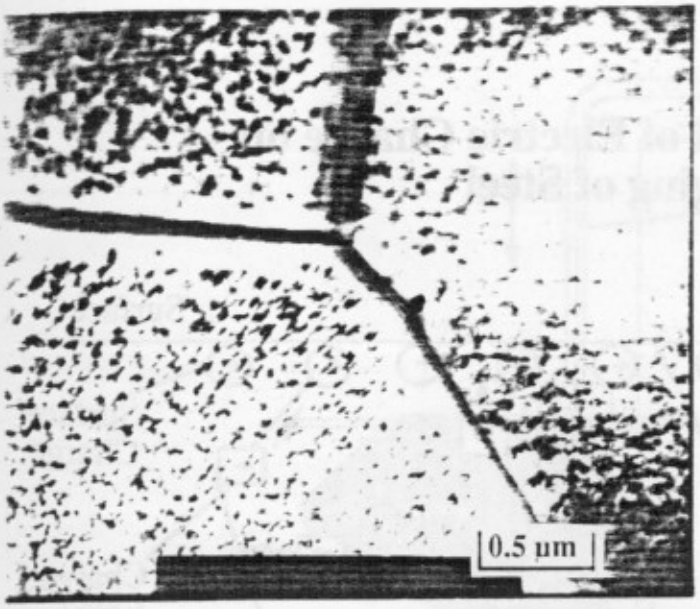

(a) 20 hrs @ 56°C

V=0

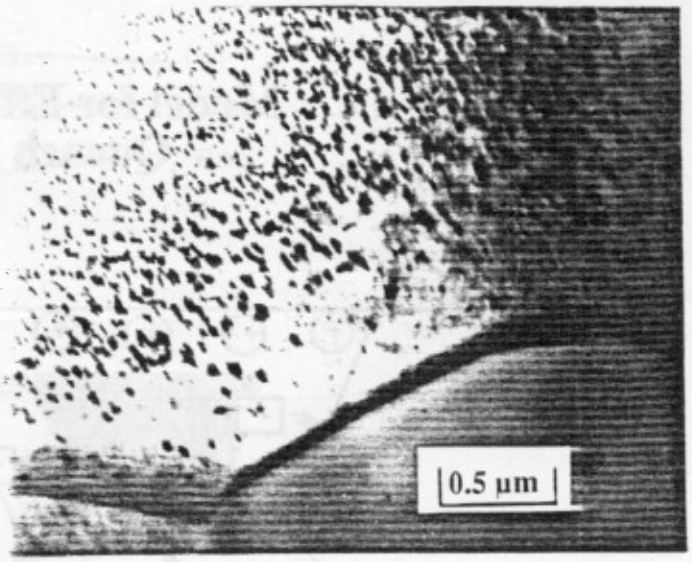

(b) 20 hrs @ 56°C

V=7 kV

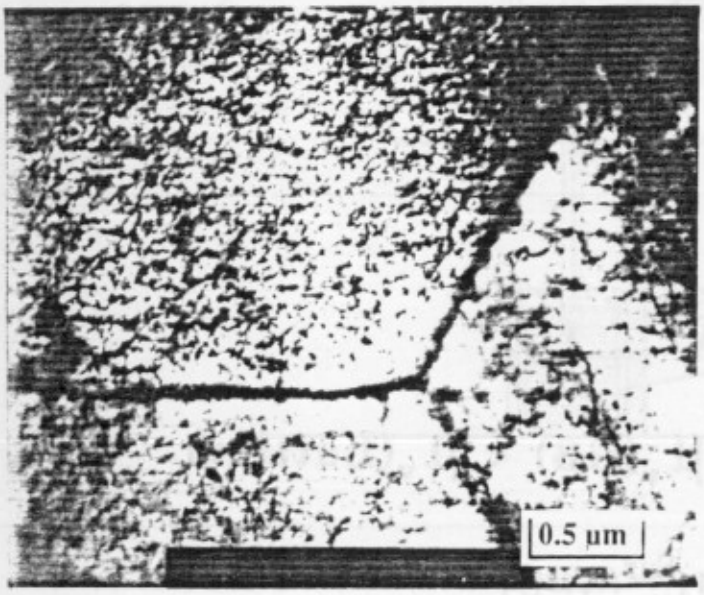

(c) 80 hrs @ 56°C

V=0

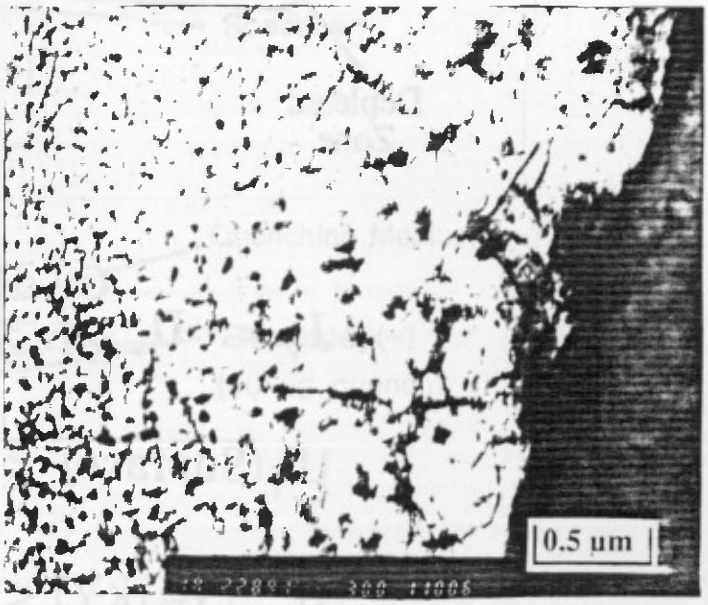

(d) 80 hrs @ 56°C

V=7 kV

Fig. 13 TEM micrographs of the precipitate structure adjacent to the grain boundaries (d = 13 µm) for aging at 56°C with E = 0 and E = 14 kV/cm: (a) and (b) t_a = 20 hr. (c) and (d) t = 80 hr.

Model for Effect of Electric Charge on Quench Aging of Steel

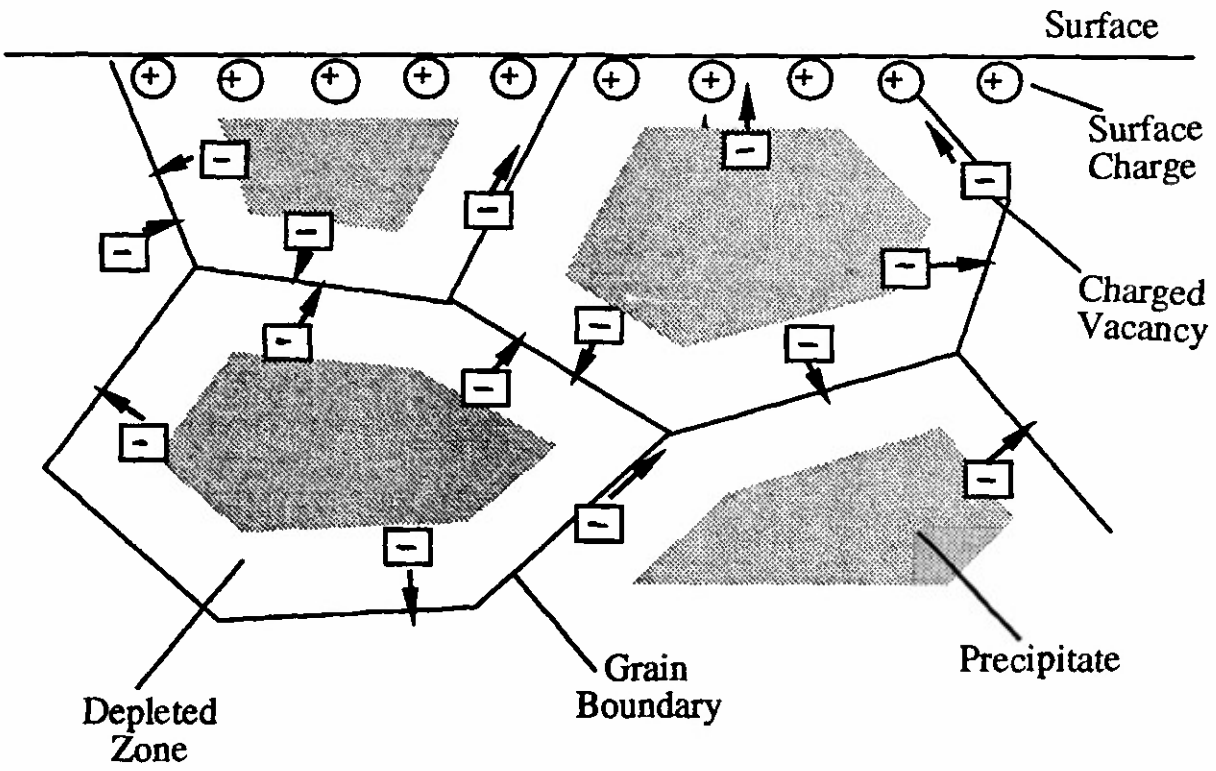

$$J_v = - D_v \frac{C_v}{kT} \frac{\partial \mu_v}{\partial X}$$

$$\mu_v(\text{Surface}) < \mu_v(\text{GB}) < \mu_v(\text{Lattice})$$

$$\mu_v^{Sur}(V=7kV) < \mu_v^{Sur}(V=0)$$

Fig. 14 Schematic of the possible influence of an electric charge produced by an external electric field on vacancy migration from the interior of the specimen to the surface thereby influencing quench aging.

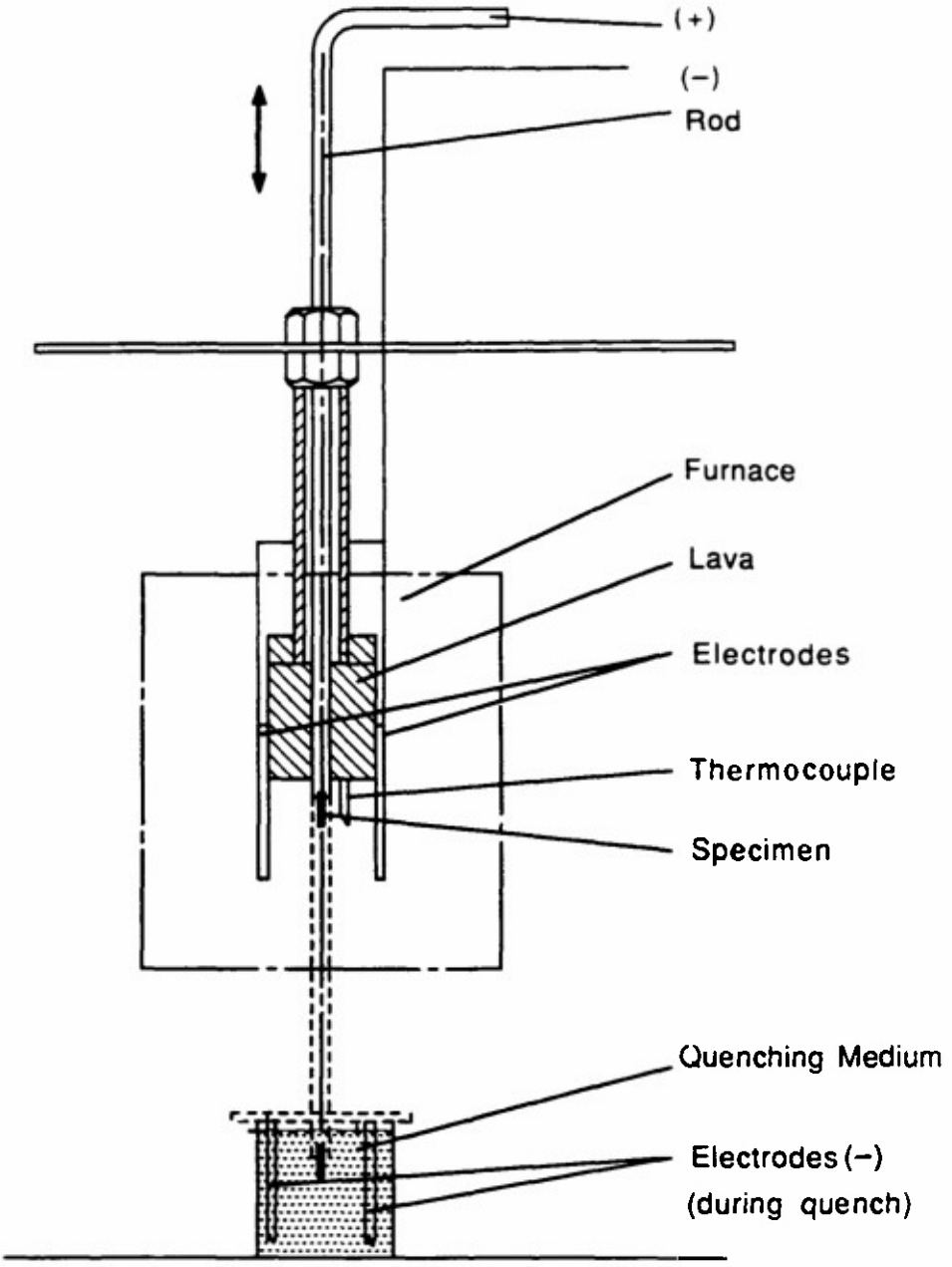

Fig. 15 Schematic of the experimental arrangement for investigating the effect of an externally applied electric field on the quench hardenability of steels.

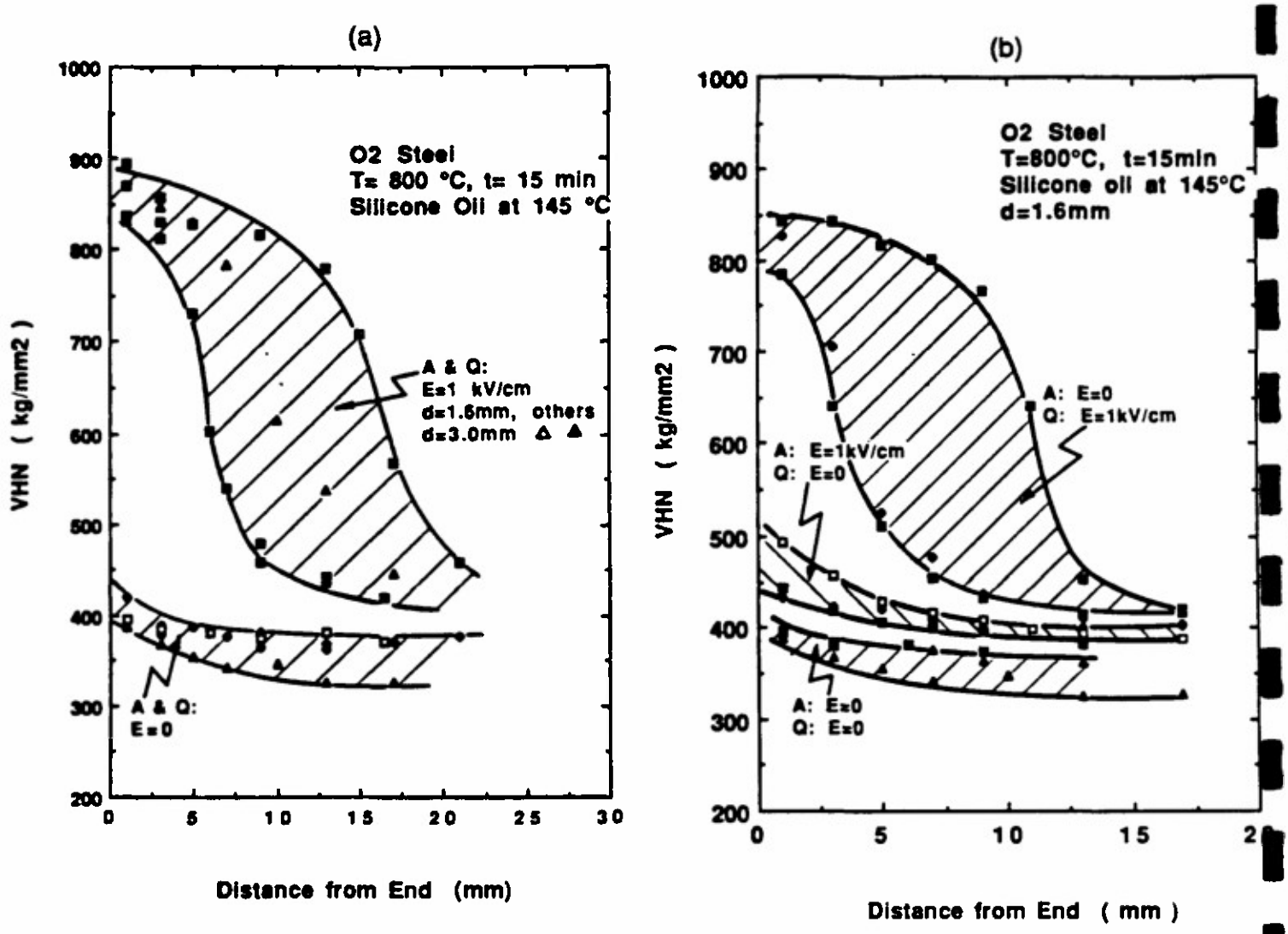

Fig. 16 Effect of an electric field on the hardness of 02 steel quenched in silicone oil at 145°C: (a) the field was applied during both austenitizing (A) and quenching (Q) and (b) the field was applied either only during austenitizing (A) or only during quenching (B).

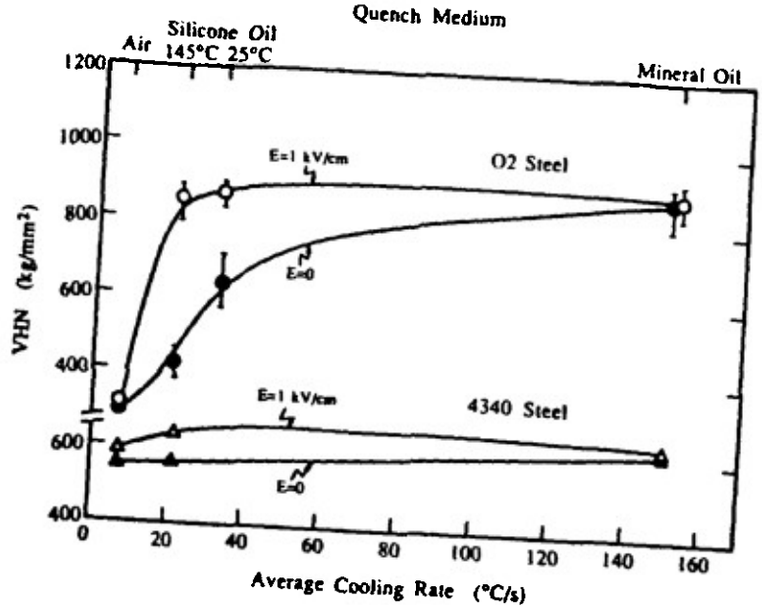

Fig. 17 The Vickers hardness at a distance of 1 mm from the tip of the specimen vs average cooling rate between 800° and 500°C for 02 steel and 4340 steel specimens.

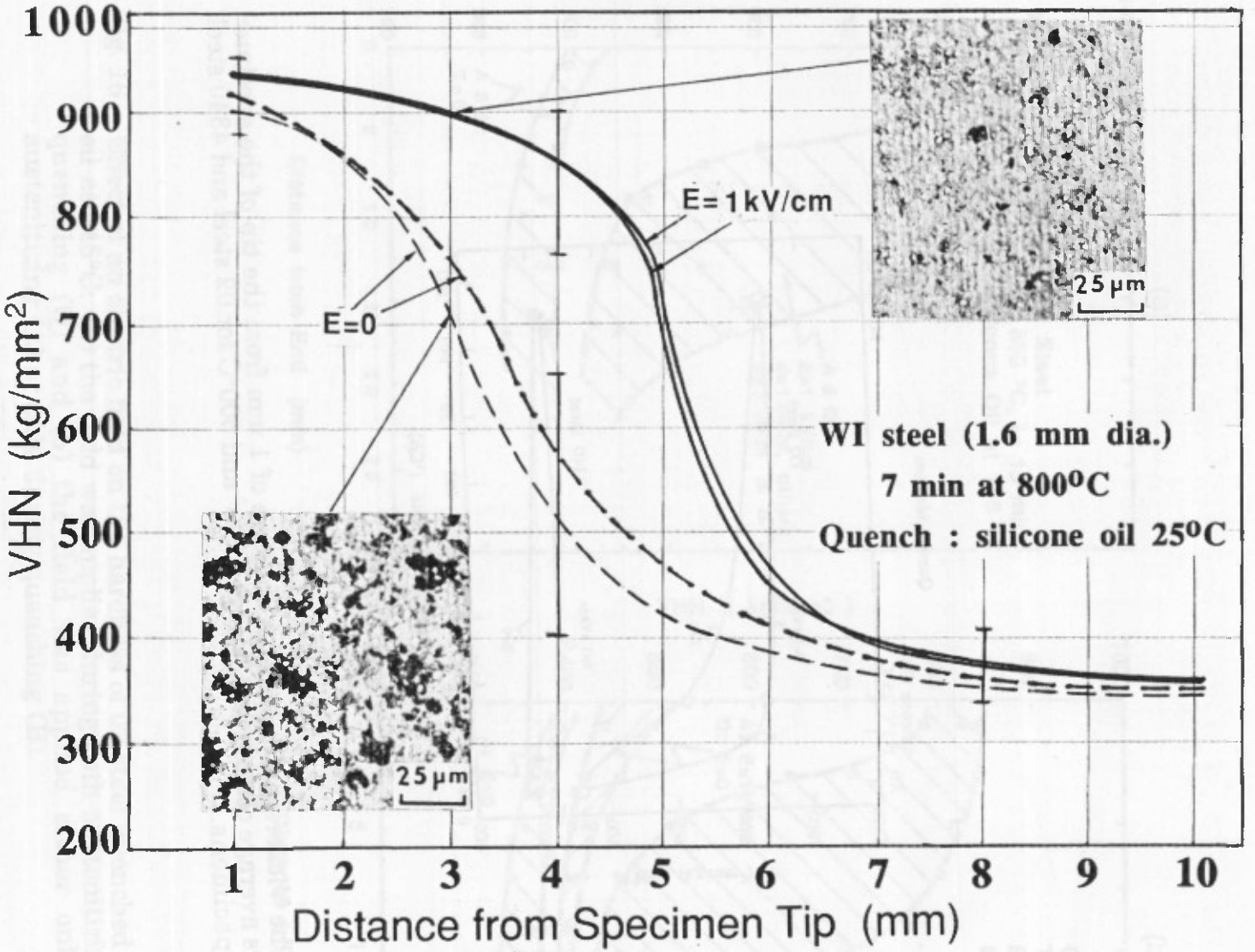

Fig. 18 Effect of an external electric field E on the hardness along 1.6 mm dia. WI tool steel specimens quenched in silicone oil at 25°C. Also shown is the microstructure at 3 mm from the quenched tip.

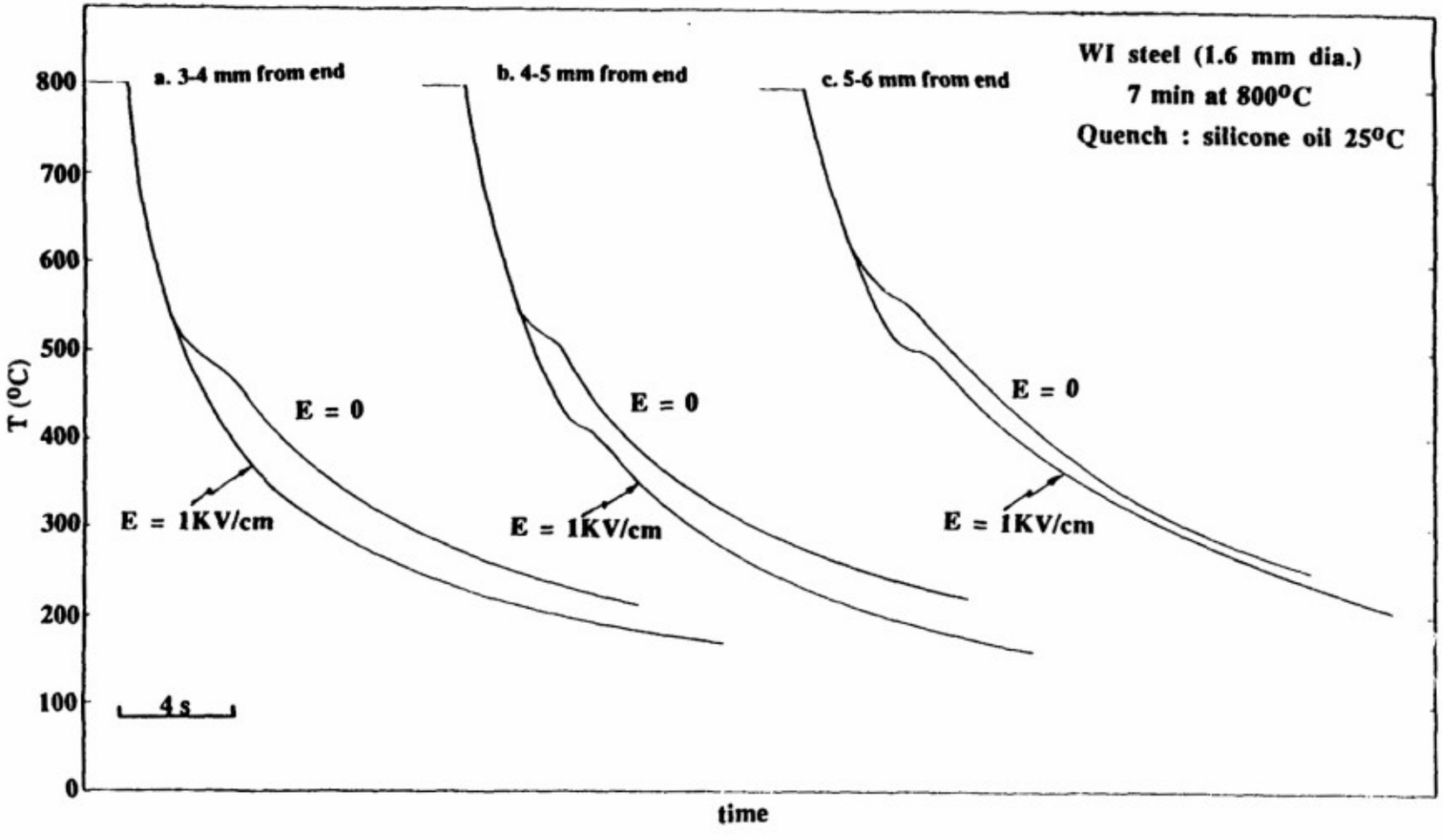

Fig. 19 Typical cooling curves with and without an electric field at three locations along the length of 1.6 mm dia. WI steel specimens.

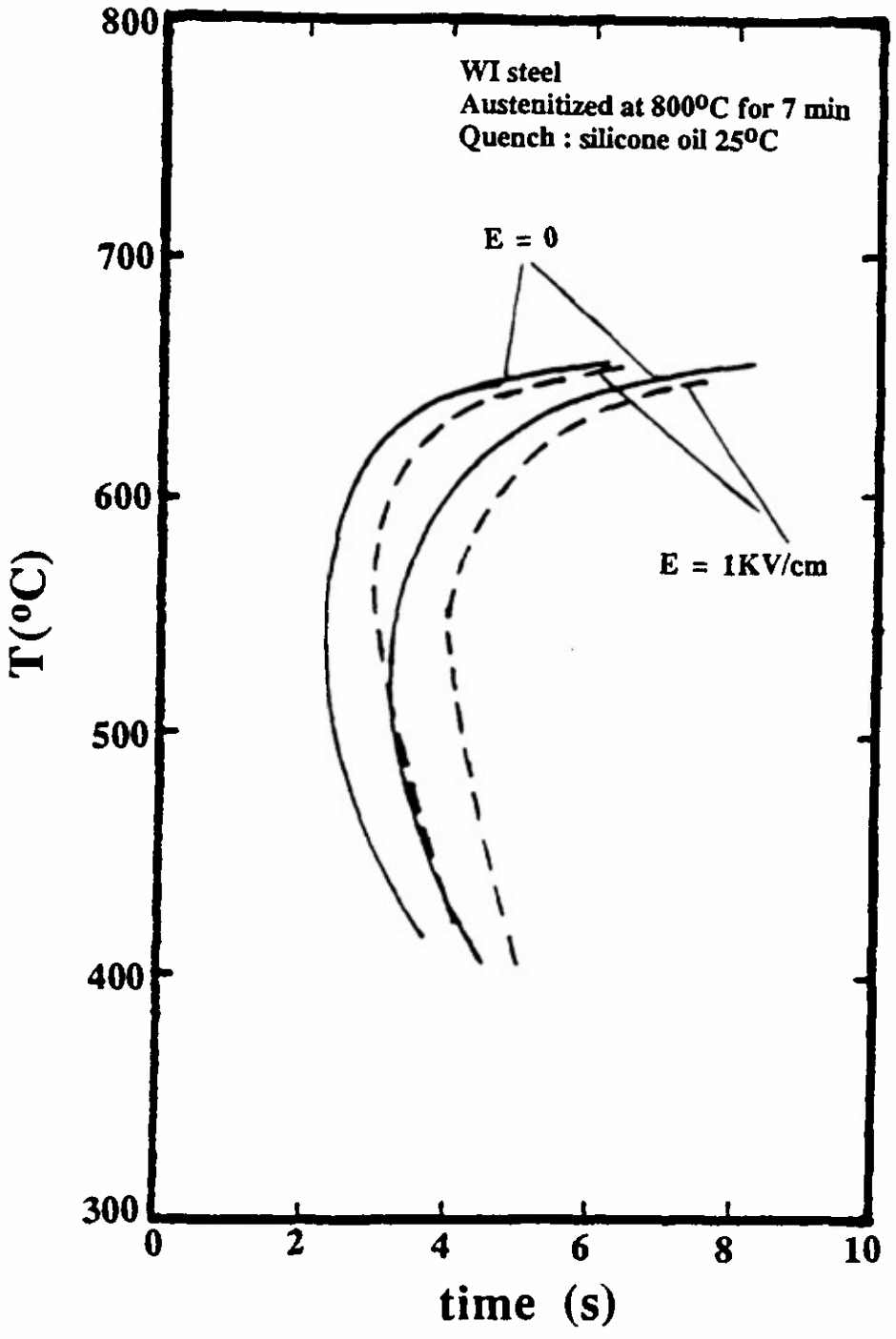

Fig. 20 Effect of electric field on the CT diagram for WI steel derived from cooling curves taken along the length of the quenched specimen.

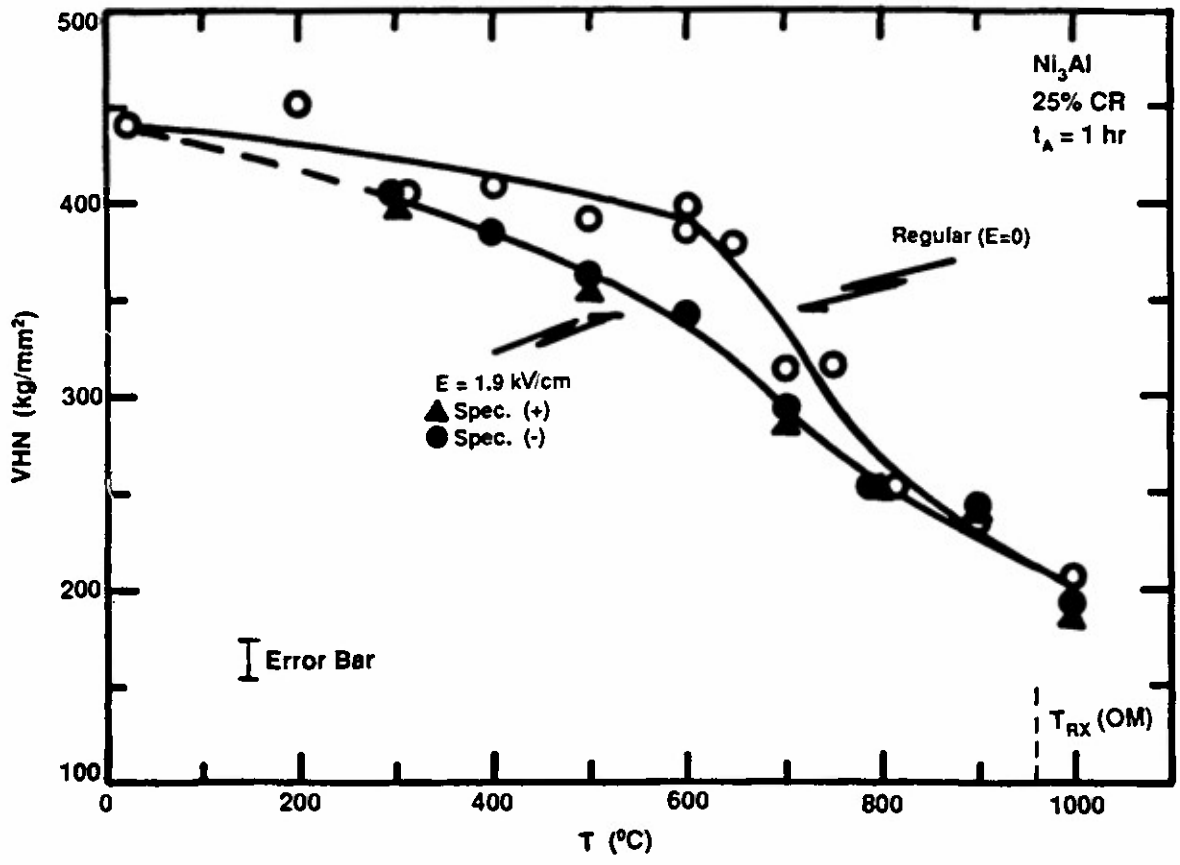

Fig. 21 Effect of an electric field of 1.9 kV/cm on the isochronal (1 hr) annealing response of Ni_3Al cold rolled 25%.

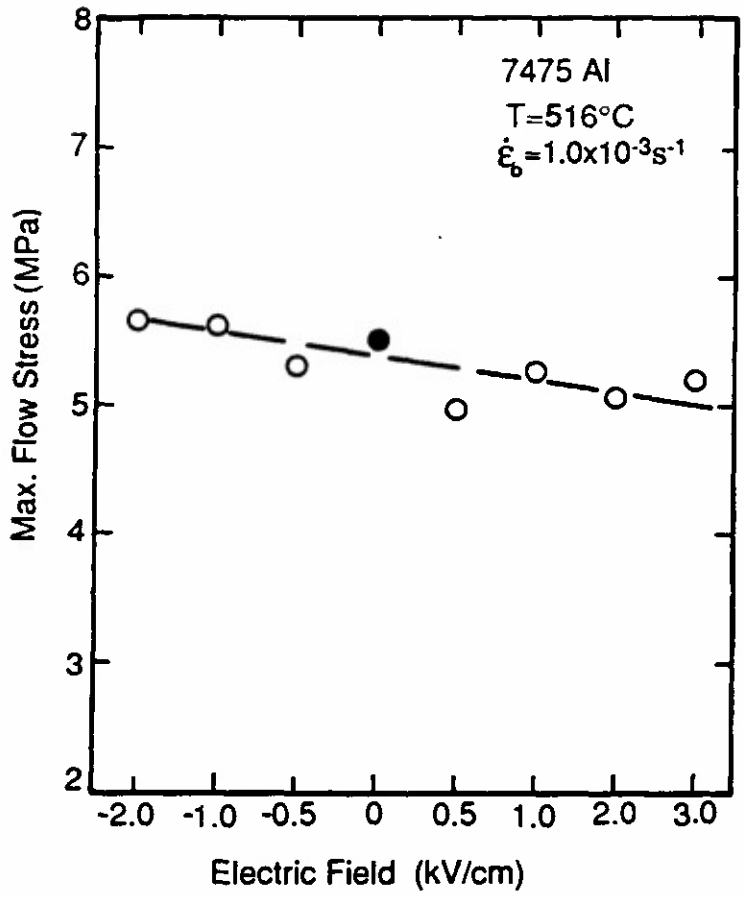

Fig. 22 Effect of polarity and magnitude of the electric field on the maximum flow stress during the superplastic deformation of 7475 Al. Positive values of the field are for specimen connected to the positive terminal of the power supply, negative values for the specimen connected to the negative terminal.

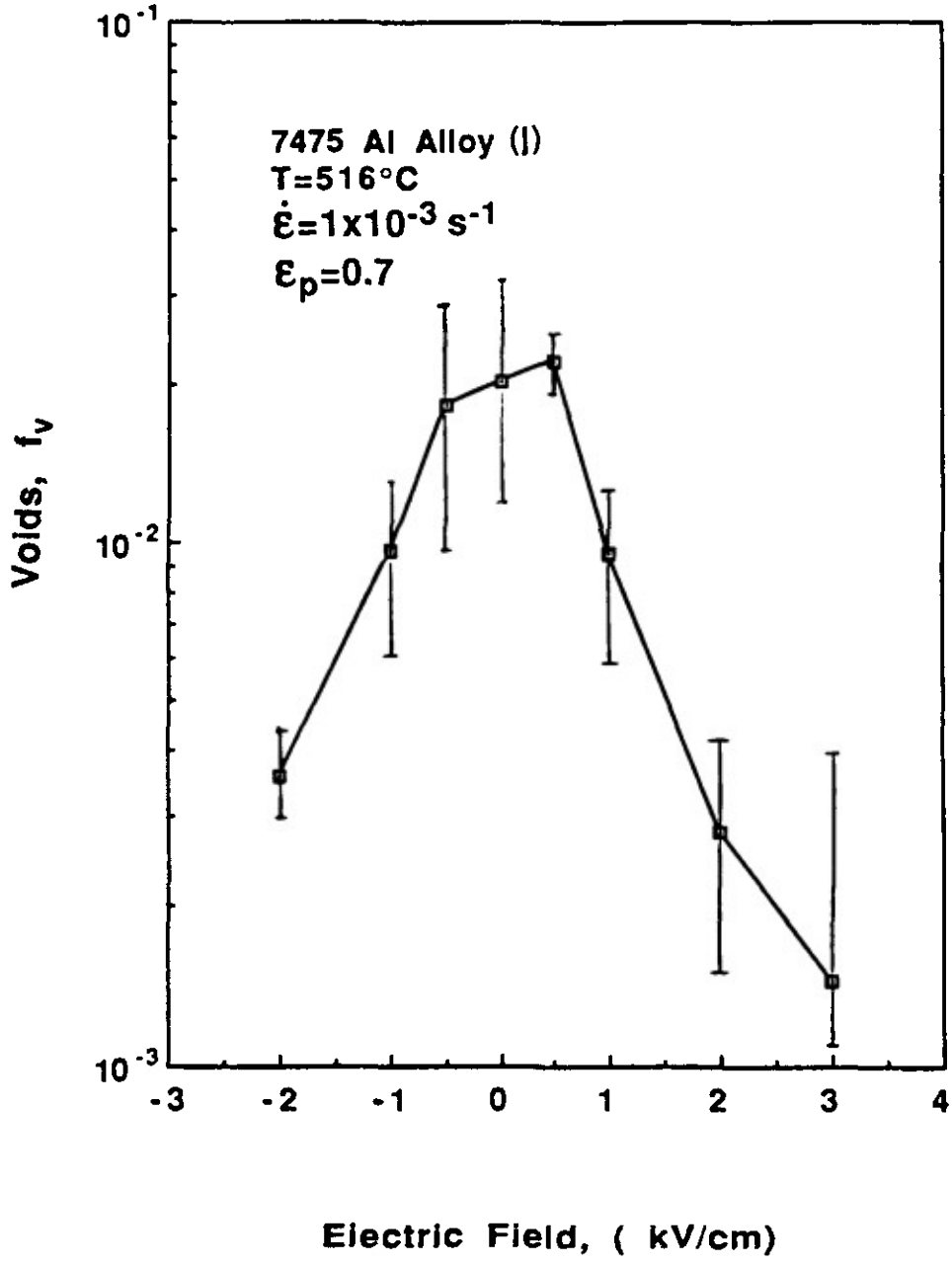

Fig. 23 Effect of polarity and magnitude of the electric field on the volume fraction of cavities in 7475 Al superplastically deformed to a true strain of 0.7 at 516°C. Positive values of the field are for specimen connected to the positive terminal of the power supply, negative values for the specimen connected to the negative terminal.

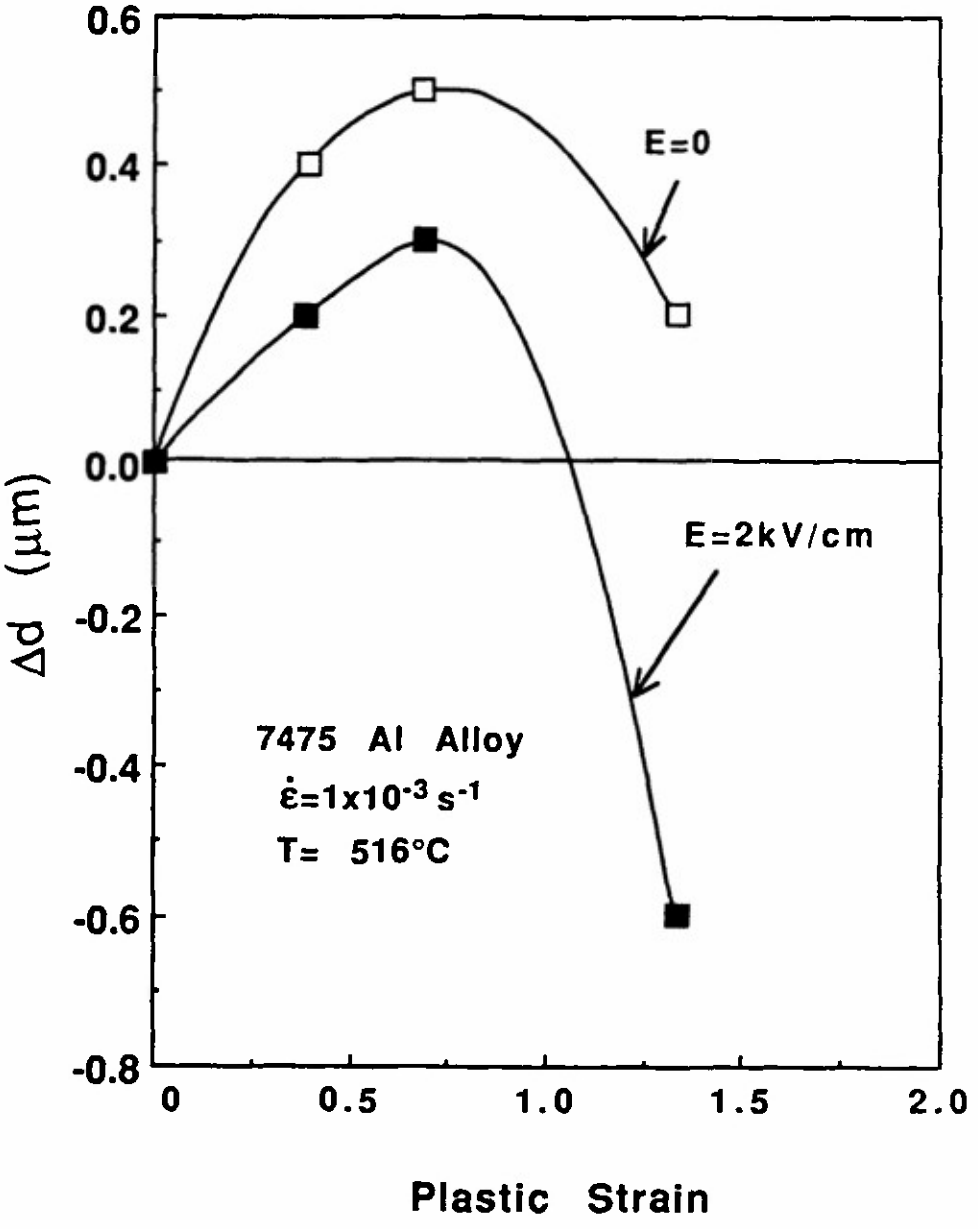

Fig. 24 Change in grain size resulting from the superplastic deformation of 7475 Al (compared to heating alone) as a function of electric field. ❑ E = 0; ■ E = 2 kV/cm.

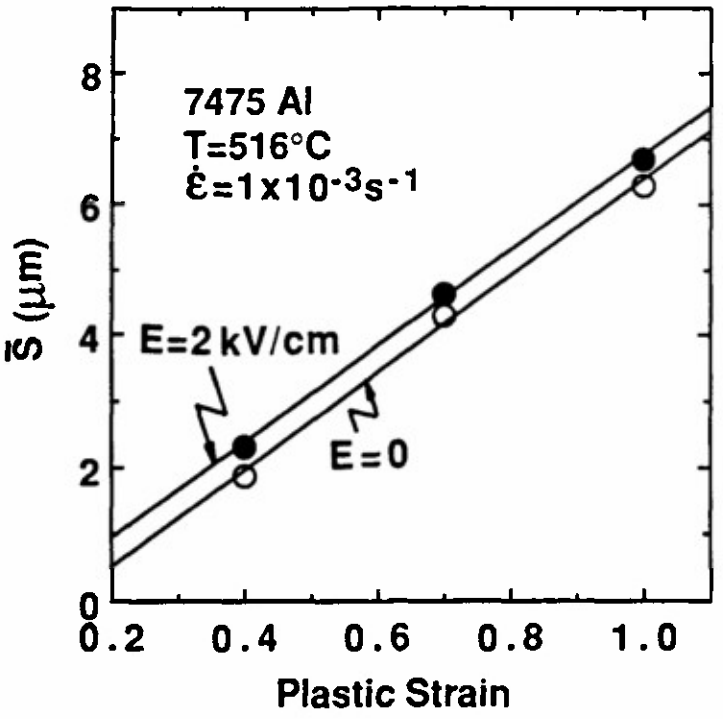

(a)

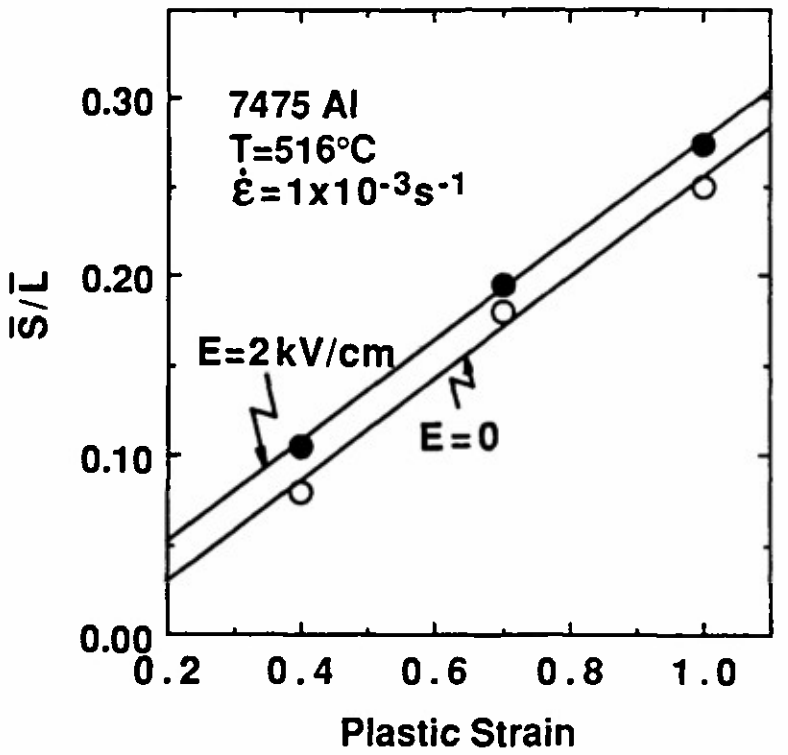

(b)

Fig. 25 Effect of an electric field of 2 kV/cm on the size of the dispersoid-free zone (DFZ) during superplastic deformation of 7475 Al: (a) mean DFZ width S vs plastic strain; (b) ratio of mean width S to mean spacing L vs plastic strain. O, E = 0; ● E = 2 kV/cm.

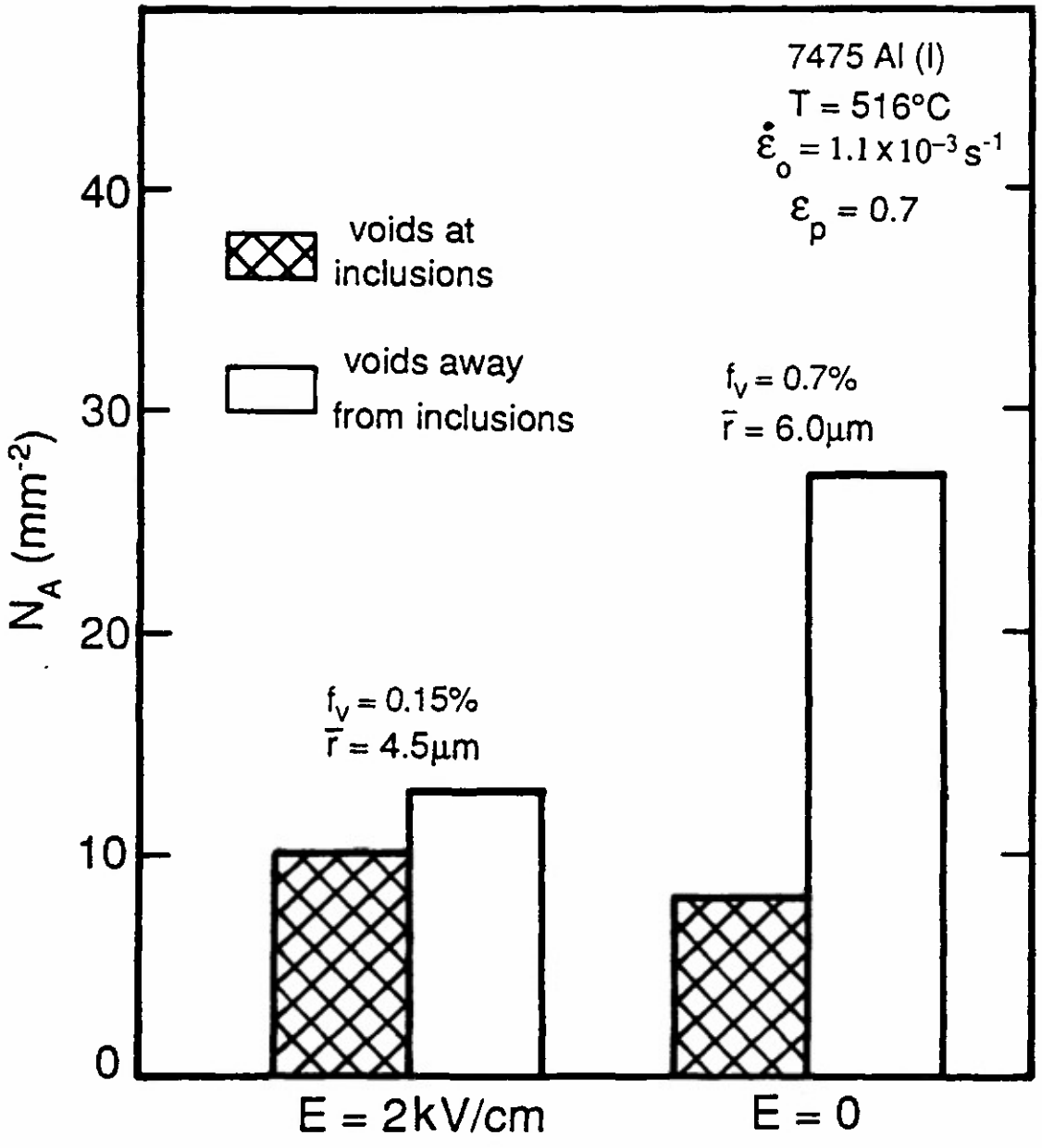

Fig. 26 Influence of an electric field of 2 kV/cm on the number of cavities per unit area N_A located along grain boundaries compared to those at inclusions for superplastic deformation of 7475 Al to a true strain of 0.7. The values of the volume fraction f_v and the average radius $\bar{r}$ of all cavities present are also given.

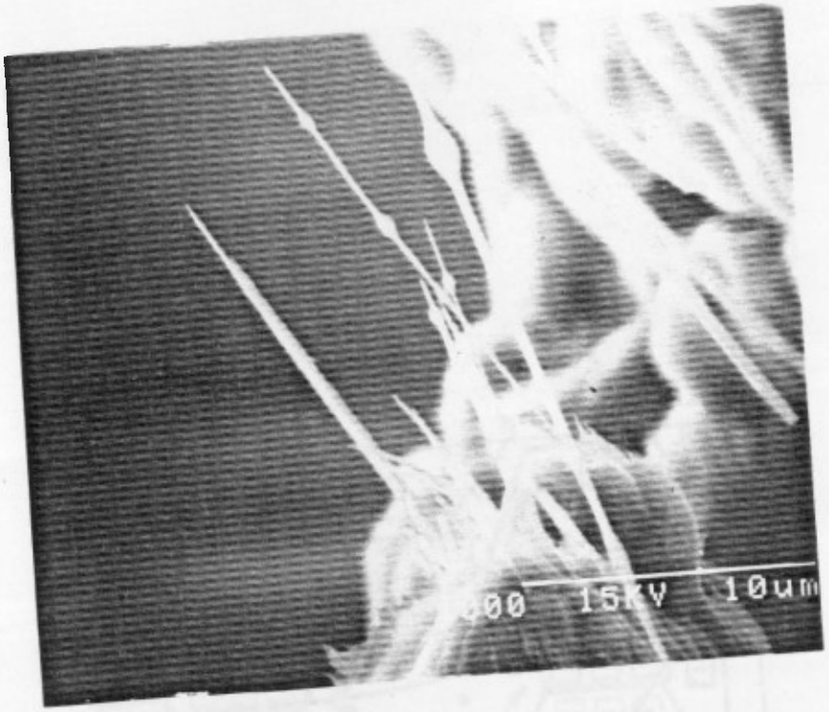

a

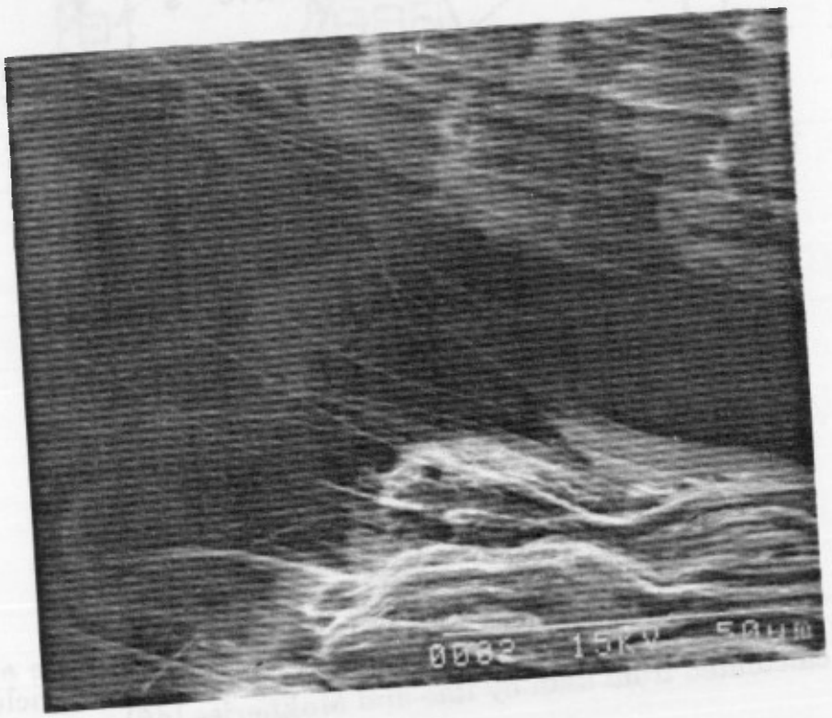

b

Fig. 27 Superplastic whiskers on the fracture surfacae of 7475 Al deformed: (a) without and (b) with and electric field at 516°C.

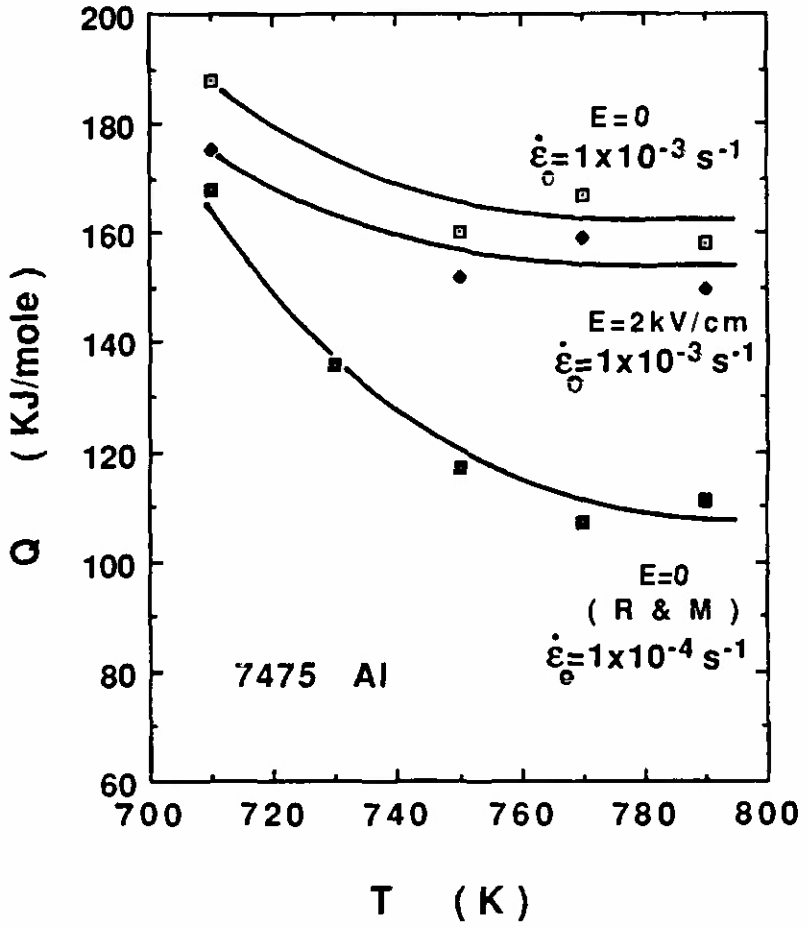

Fig. 28 Effect of electric field on the temperature dependence of the activation energy for the superplastic deformation in 7475 Al. Also included are values calculated from data by Rao and Mukherjee [46].

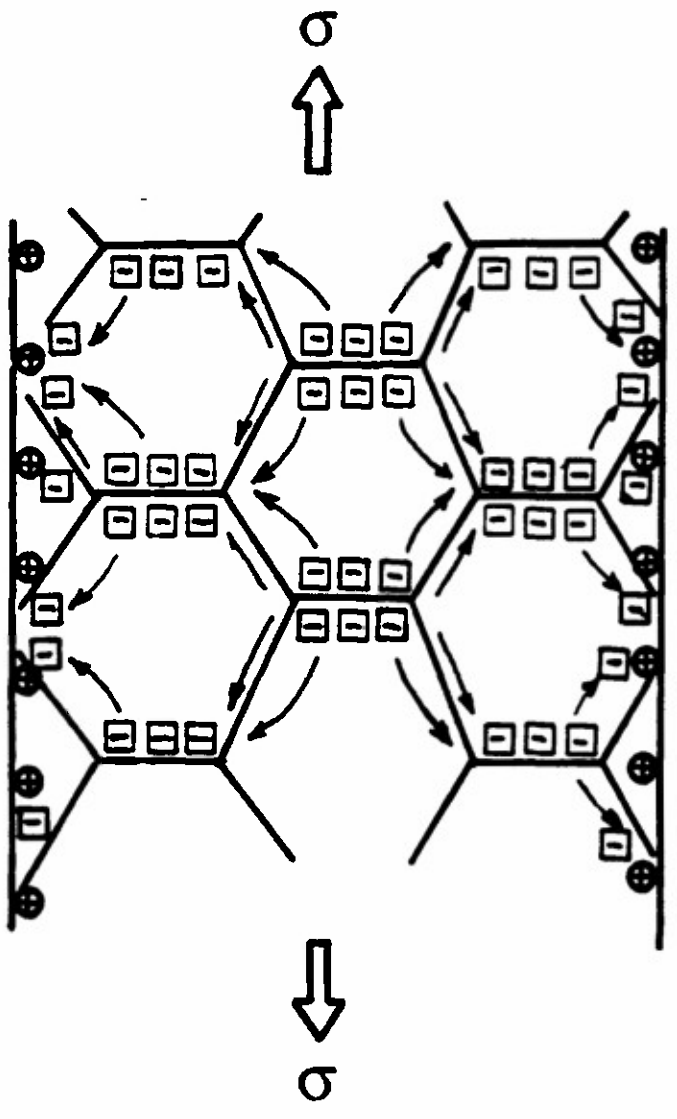

Fig. 29 Schematic of possible mechanism for the effect of an electric field on the superplastic deformation of 7475 Al.

APPENDIX

Scientific Papers, Reports, Student Theses, News Coverage, Interactions with Industry and Government and International Association

Scientific Papers

I. Influence of Electric Circuit

A. Plastic Deformation

1. H. Conrad, W. D. Cao and A. F. Sprecher, "Constitutive Laws Pertaining to Electroplasticity in Metals", in Constitutive Laws of Plastic Deformation and Fracture, A. S. Krausz et al (eds.), Kluwer Academic Publ., Netherlands (1990) p. 305–311.
2. W. D. Cao, A. F. Sprecher and H. Conrad, "Measurement of the Electroplastic Effect in Nb", J. Phys. E: Sci. Instrum 22 (1989) 1026–1034.
3. W. D. Cao, A. F. Sprecher and H. Conrad, "The Electroplastic Effect in Niobium", in High Temperature Niobium Alloys, J. J. Stephens and I. Ahmad (eds.), TMS, Warrendale, PA (1991) p. 27–47.
4. H. Conrad, A. F. Sprecher, W. D. Cao and X. P. Lu, "Electroplasticity — The Effect of Electricity on the Mechanical Properties of Metals", Jnl. Met. 42 (Sept. 1990) 28–33.

B. Fatigue

1. H. Conrad, J. White, W. D. Cao, X. P. Lu and A. F. Sprecher, "Effect of Electric Current Pulses on Fatigue Characteristics of Polycrystalline Copper, Mat. Sci. Engr. A145 (1991) 1–12.
2. W. D. Cao and H. Conrad, "On the Effect of Persistent Slip Band (PSB) Parameters on Fatigue Life", Fatigue Fract. Mater. Struct. 15 (1992) 573–583.
3. Z. H. Lai, C. X. Ma and H. Conrad, "Cyclic Softening by High Density Electric Current Pulses During Low Cycle Fatigue of a-Ti"; Scripta Met. Mat. 27 (1992) 527–531.

C. Annealing

1. H. Conrad, Z. Guo and A. F. Sprecher, "Effects of Electropulse Duration and Frequency on Grain Growth in Cu", Scripta Met. Mat. 24 (1990) 359–362.

2. H. Conrad, Z. Guo, M. Fisher, W. D. Cao and A. F. Sprecher, "Effects of Electric Current Pulses on the Recrystallization of Metals", in Recrystallization '90, T. Chandra (ed.), TMS, Warrendale, PA (1990) p. 301–306.

D. Phase Transformations

1. Z. H. Lai, H. Conrad, Y. S. Chao, S. Q. Wang and J. Sun, "Effect of Electropulsing on the Microstructure and Properties of Iron-Based Amorphous Alloys", Scripta Met. 23 (1989) 305–310.

II. Influence of An External Electric Field

A. Phase Transformations

1. W. D. Cao, X. P. Lu, A. F. Sprecher and H. Conrad, "Increased Hardenability of Steel by an Electric Field", Mat. Lettr. 9 (1990) 193–197.
2. H. A. Lu and Hans Conrad, "Influence of an Electric Charge During Quench-Aging of a Low-Carbon Steel, Appl. Phys. Lett. 59 (1991) 1847–1849.
3. H. Conrad, Y. Chen and Hao An Lu, "The Influence of an Electric Charge on the Quench Aging of a Low-Carbon Steel", in Int. Symp. Microstructures and Properties of Aging Materials, TMS-ASM (Chicago, 4 Nov., 1992) in print.

B. Superplastic Deformation

1. W. D. Cao, X. P. Lu, A. F. Sprecher and H. Conrad, "Superplastic Deformation Behavior of 7475 Aluminum Alloy in an Electric Field", Mater. Sci. Engr. A129 (1990) 157–166.
2. W. D. Cao, X. P. Lu, A. F. Sprecher and H. Conrad, "Superplastic Behavior and Microstructure of 7475 Al Deformed in an External Electric Field", in Superplasticity in Aerospace II, T. R. McNelley and H. C. Heikkenen (eds.), TMS, Warrendale, PA (1990) p. 269–283.
3. H. Conrad, W. D. Cao, X. P. Lu and A. F. Sprecher, "Effect of Electric Field on Cavitation in Superplastic Aluminum Alloy 7475", Mater. Sci. Engr. A138 (1991) 247–258.
4. X. P. Lu, W. D. Cao, A. F. Sprecher and H. Conrad, "Influence of an External Electric Field on the Microstructure of Superplastically Deformed 7475Al", J. Mater. Sci. 27 (1992) 2243–2250.

III. Related Research

1. A. Zayed and H. Conrad, "Evaluation of the Parameters Which Govern Local Necking in 3003–0 Al Sheet", NAMRC-XX, Washington State Univ. (May 20–22, 1992) in print.

Student Theses

1. James Campbell, "The Effects of d.c. and a.c. Current on the Quench Aging of a Low-Carbon Steel", expected May, 1993.

Reports

1. H. Conrad and I Ahmad, eds., "High-Intensity Electro-Magnetic and Ultrasonic Effects on Inorganic Materials Behavior and Processing", U. S. ARO Workshop, North Carolina State University, July 17–18, 1989.
   (a) H. Conrad, A. F. Sprecher, W. D. Cao and X. P. Lu, "Effects of Electric Current and External Electric Field on the Mechanical Properties of Metals-Electroplasticity".
   (b) A. F. Sprecher and H. Conrad, "Effects of an Electric Current and External Electric Field on the Annealing of Metals".
   (c) H. Conrad, A. F. Sprecher, W. D. Cao and X. P. Lu, "Effects of Electric Fields and Currents on Phase Transformations in Bulk Alloys".
   (d) A. F. Sprecher and H. Conrad, "Application of Electroplasticity in Metal Working — Review of Soviet Work".
   (e) D. Kuhlman-Wilsdorf and H. Conrad, "Thoughts on Possible Explanations for the Various Observations Presented at the Workshop".
   (f) H. Conrad, "Issues and Opportunities".
2. H. Conrad, "Review of Research on the Influence of Electric Fields and Currents on the Behavior of Metals and Alloys", Materials Sci. & Engr. Dept., N. C. State Univ., Raleigh, N. C., Feb. 1, 1990.
3. H. Conrad and A. F. Sprecher, "Effects of Electric Fields and Currents on Microstructure", Properties and Processing of Metals and Alloys: Summary of Research at North Carolina State University", Mat. Sci. Engr. Dept., N. C. State Univ., Raleigh, N. C., July 1, 1990.

News Coverage

A. Print

1. "Electric Field Process Metal", Inside R & D, 18 No. 32 (Aug. 9, 1989).

2. "A Hot Breakthrough May Add Muscle to Metal", Business Week: Science and Technology Section, (Aug. 14, 1989) p. 89.
3. "An Electrifying Discovery", Of Material Interest, Adv. Mater. Processes (Oct. 1989) p. 6.
4. "Discovery Might Lead to Improved Strength, Heat Resistance and Toughness of Metals", Jnl. of Metals, News and Update, (Oct. 1989) p. 4.
5. "Electric Fields Put Metals into a Better Temper", New Scientist (Sept. 1989) p. 35.
6. "Quenching Method Penetrates Steel, Doubles Its Strength", R & D Magazine, News Section, Processes (Feb. 1990) p. 60.
7. J. J. Gilman and J. H. Westbrook, Physics Today Letters, (Apr. 1990) p. 15.
8. "Electric Field Enhancement of Metals", Futurtech, No. 106 (May 29, 1990).
9. "Electric-Field Enhancement of Metals", AMT's Strategic Technologies (July 15, 1990) p. 9.
10. "Federn Veränderin Metalk", Welt, Technik Section (July 28, 1990) p. 20.

B. T. V. — National and International
1. "Novel Effect of an Electric Field on the Properties of Metals", CNN Science and Technology Series, Feb. 1989.
2. "Effects of an Electric Field on the Properties of Metals", Educational Channel 4 Series on Research at North Carolina State University, Feb. and Apr., 1992.

Interactions With Industry and Government

A. Exploratory studies were performed for three large industrial firms on the following subjects:
1. Effects of an external electric field on superplasticity
2. Electro-compaction of Al alloy composites.

B. Organized with I. Ahmad of U. S. ARO a workshop "High-Intensity Electromagnetic and Ultrasonic Effects on Inorganic Materials Behavior and Processing", N. C. State Univ., July 17–18, 1989.

International Association

H. Conrad has been appointed Vice President of the Association of Intensive Electrotechnology of Materials Processing, headquartered in Moscow, Russia.